People's Democratic Republic of Algeria
Ministry of Higher Education and Scientific Research
University of Cheikh Larbi Tebessi - Tebessa
Faculty of Exact Sciences, Natural Sciences and Life Sciences
Department of Mathematics

Presented for the award of the Master's degree in Mathematics - Dynamical Systems and Its Applications

Synchronization of Chaos in Discrete Dynamical Systems

By: Abdelbari Radjai

Under the direction of professors: Boukhalfa El-hafsi and Nouioua Tarek

Discussed by the committee:

Mme. Gasri Ahlem	MCA	University of Cheikh Larbi Tebessi	*President*
Mr. Toualbia Abdellatif	MCB	University of Cheikh Larbi Tebessi	*Examiner*
Mr. Boukhalfa El Hafsi	MCB	University of Cheikh Larbi Tebessi	*Supervisor*
Mr. Nouioua Tarek	MCB	University of Cheikh Larbi Tebessi	*Supervisor*

Year: 2024/2025

Acknowledgments

In the name of Allah, the Most Gracious, the Most Merciful.

Alhamdulillah for His countless blessings.

I am sincerely thankful for the guidance and support I have received from *El Hafsi Boukhalfa* and *Tarek Nouioua*, my supervisors.

I would like to thank the staff of the Department of Mathematics at the University of Cheikh Larbi Tebessi – Tebessa, for welcoming me into a hardworking environment and providing the necessary academic support to complete this research.

Above all, I owe my deepest gratitude to my father, *Toufik Radjai*. No one could ever imagine the sacrifices he made or the love he gave me. His belief in me has always been and continues to be the fuel that keeps me going. This thesis is as much his as it is mine. I hope it makes you proud of me, as I have always been proud to be your son.

A special mention goes to the one who gives selflessly without ever expecting anything in return, to the first teacher, the best friend, the quiet supporter, and the eternal source of love. Thank you, Mom. I love you.

I am also deeply grateful to my sisters for their endless, unconditional love, care, and support. This achievement belongs to all of us.

To my colleagues and friends, thank you for making each day enjoyable.

And there's no better ending than the iconic thanks inspired by *Snoop Dogg* himself:

> *"Last but not least, I wanna thank me.*
> *I wanna thank me for believing in me.*
> *I wanna thank me for doing all this hard work.*
> *I wanna thank me for having no days off.*
> *I wanna thank me for, for never quitting.*
> *I wanna thank me for always being a giver.*
> *And tryna give more than I receive.*
> *I wanna thank me for tryna do more right than wrong.*
> *I wanna thank me for just being me at all times."*

Abstract

The objective of this thesis is to present the problem of chaos synchronization. More specifically, we are interested in the synchronization of discrete nonlinear dynamical systems, whose formulations are given by recurrent functions with the presence of bifurcation parameters, where a small perturbation in the initial conditions results in a large discrepancy between long-term observations.
The unification of observations of two long-term phenomena is equivalent to the synchronization of their representative dynamical systems from a certain rank (time) by applying the various types of synchronization cited in the literature, including Complete Synchronization, Anti-Synchronization, Phase Synchronization, Lag Synchronization, Generalized Synchronization, Projective Synchronization, FSHP Synchronization, and Q-S Synchronization.

Resumé

L'objectif de cette thèse est de présenter le problème de la synchronisation chaotique. Plus précisément, nous nous intéressons à la synchronisation de systèmes dynamiques non linéaires discrets, dont les formulations sont données par des fonctions récurrentes avec présence de paramètres de bifurcation, où une faible perturbation des conditions initiales entraîne une grande divergence entre les observations à long terme.
L'unification des observations de deux phénomènes à long terme équivaut à la synchronisation de leurs systèmes dynamiques représentatifs à partir d'un certain rang (temps) en appliquant les différents types de synchronisation cités dans la littérature, notamment la synchronisation complète, l'antisynchronisation, la synchronisation de phase, la synchronisation de retard, la synchronisation généralisée, la synchronisation projective, la synchronisation FSHP et la synchronisation Q-S.

Introduction

Simultaneously with the research on chaos in discrete dynamical systems, a line of mathematical investigation has evolved in parallel, focusing on the *synchronization of chaotic motions*, a topic that has drawn considerable interest from numerous researchers. Among the pioneers in this area are Yamada and Fujisaka [30], who introduced a local approach to chaotic synchronization. Subsequently, Afraimovich *et al.* [1] developed foundational concepts of chaotic synchronization, which were later expanded upon by Pecora and Carroll [24], who defined what is now known as *identical synchronization*. Their approach was based on coupled chaotic circuits, structured such that one system acted as the *master* and the other as the *slave*.
A more recent framework, known as *generalized synchronization*, was introduced by Rulkov *et al.* [26]. Due to their applicability in telecommunications, secure information transmission [31], and cryptography [3], discrete chaotic dynamical systems have gained increasing importance. This is further reinforced by the fact that numerous mathematical models of physical processes, biological systems, chemical reactions, and economic phenomena [20] [17] are effectively described by discrete dynamical systems. Consequently, the study of *synchronization in discrete chaotic systems* has become a significant area of contemporary research.

In this context, our thesis is organized into four essential and interconnected chapters. The first chapter is dedicated to the general theory of discrete dynamical systems, including fundamental definitions related to the state space, dynamical rules, fixed points along with their classification and stability, as well as bifurcation theory. In the second chapter, we discuss the tools for measuring and quantifying chaos. Then in the third chapter we illustrate the manifestation of chaos in discrete dynamical systems through classical examples of *universal discrete chaotic maps*, both in the plane and in higher-dimensional settings. Finally, the fourth chapter focuses on the various types of synchronization phenomena observable in discrete dynamical systems, along with the mathematical methods used to analyze and achieve them.

List of Figures

1.1 Saddle-Node Bifurcation Diagram 11
1.2 Transcritical Bifurcation Diagram 12
1.3 Pitchfork Bifurcation Diagram 12
1.4 Period-Doubling Bifurcation Diagram 13
1.5 Neimark-Sacker Bifurcation Diagram with Prey Refuge Effect 13
1.6 Crisis Bifurcation Diagram 14
1.7 Border-Collision Bifurcation and its Map Function Plots. 15

3.1 Logistic Map Attractor for $r = 3.9$. 22
3.2 Logistic Map – First 100 Iterations of x_n 23
3.3 Logistic Map Bifurcation Diagram for $x_0 = 0.4$ 24
3.4 Logistic Map : Lyapunov Exponent Evolution 24
3.5 Hénon Strange Attractor for $a = 1.4$, $b = 0.3$. 25
3.6 Hénon Map – First 100 Iterations of x_n 26
3.7 Hénon Map Bifurcation Diagram for $b = 0.3$. 26
3.8 Hénon Map : Lyapunov Exponent Evolution 27
3.9 Lozi Strange Attractor for $a = 1.7$, $b = 0.5$. 28
3.10 Lozi Map – First 100 Iterations of x_n. 29
3.11 Lozi Map Bifurcation Diagram for $b = 0.5$. 29
3.12 Lozi Map : Lyapunov Exponent Evolution 30
3.13 Lorenz Strange Attractor for $a = 1.25$, $b = 0.75$. 31
3.14 Lorenz Map – First 100 Iterations of x_n. 32
3.15 Lorenz Map Bifurcation Diagram for $a \in [0, 2]$, $b = 0.75$. 32
3.16 Lorenz Map : Lyapunov Exponent Evolution 33

4.1 Complete Synchronization Diagram 37
4.2 Anti Synchronization Diagram 39
4.3 Phase Synchronization Diagram 41
4.4 Lag Synchronization Diagram 42
4.5 Generalized Synchronization Diagram 44
4.6 Projective Synchronization Diagram 46
4.7 FSHP Synchronization Diagram 48
4.8 Q-S Synchronization Diagram 50

Contents

Acknowledgment **1**

Abstract **2**

Introduction **3**

1 Preliminaries on Discrete Dynamical Systems **7**
1.1 General Concepts 7
1.1.1 Discrete Dynamical Systems 7
1.1.2 Orbits 7
1.1.3 Equilibrium Points 8
1.1.4 Periodic Orbits of Order p (p-Cycles) 8
1.1.5 Phase Space 8
1.2 Stability 8
1.2.1 Lyapunov Stability and Asymptotic Stability 9
1.2.2 Linearization 9
1.2.3 Nature of Equilibrium via Linearization 9
1.2.4 Lyapunov Function 10
1.3 Bifurcation Theory in Discrete Systems 10
1.3.1 Definition of Bifurcation 10
1.3.2 Role of Bifurcations in Chaos 11
1.3.3 Fundamental Types of Bifurcations 11
1.3.4 Bifurcations Leading to Chaos 13
1.3.5 Special Case in Non-Smooth Systems 14
1.4 Summary 16

2 Chaos Quantification Tools **17**
2.1 Chaos in Discrete Systems 17
2.1.1 Lyapunov Exponents: Measuring Sensitivity to Initial Conditions . . 18
2.1.2 Feigenbaum's Constants 20
2.1.3 Fractal Dimensions and Strange Attractors in Discrete Maps 21
2.2 Summary 21

3 Key Discrete Chaotic Maps **22**
3.1 Logistic Map 22
3.2 Hénon Map 25
3.3 Lozi Map 28
3.4 Lorenz Map 31
3.5 Summary 34

4 Synchronization of Chaos in Discrete Dynamical Systems **35**

4.1 The Concept of Chaos Synchronization 35
4.2 Definition and Importance of Synchronization 35
4.3 Types of Synchronization 36
4.3.1 Complete Synchronization 36
4.3.2 Anti-Synchronization 38
4.3.3 Phase Synchronization 40
4.3.4 Lag Synchronization 42
4.3.5 Generalized Synchronization 43
4.3.6 Projective Synchronization 45
4.3.7 Full State Hybrid Projective Synchronization (FSHPS) 47
4.3.8 Q-S Synchronization 49
4.4 Methods of Synchronization 51
4.4.1 Active Controller Method 51
4.4.2 Adaptive Controller Method 53
4.5 Summary 55

Chapter 1

Preliminaries on Discrete Dynamical Systems

This chapter establishes the foundational concepts necessary for the study of discrete dynamical systems. It introduces the mathematical formulation of such systems, their orbits, and the classification of equilibrium and periodic behavior. Stability is rigorously treated through Lyapunov methods and linearization, including the Hartman–Grobman theorem. The role of bifurcations in the emergence of complex dynamics, particularly chaos, is examined with emphasis on key bifurcation types. These preliminaries are essential for understanding chaotic behavior and synchronization in later chapters.

1.1 General Concepts

This section presents the core mathematical elements of discrete dynamical systems, including their formal definition, orbit structure, and the classification of fixed and periodic points. It also introduces the notion of phase space as the framework within which system evolution is visualized and analyzed. These concepts are foundational for characterizing dynamical behavior across parameter regimes.

1.1.1 Discrete Dynamical Systems

Definition 1.1. [10] Consider a system of recurrent algebraic equations

$$x_{k+1} = f(x_k; \Gamma), \quad k \in \mathbb{N}, \tag{1.1}$$

which defines a discrete dynamical system where $x_k \in \mathbb{R}^n$ is the state vector at the k-th iteration, $\Gamma \in \mathbb{R}^m$ (with $m \geq 1$) is the parameter vector, and f is the nonlinear recurrence function which dictates the dynamics of the system.

1.1.2 Orbits

Definition 1.2. [10] The orbit of a point x_0 under the system (1.1) is given by:

$$O(x_0) = \{x_0, f(x_0), f^2(x_0), f^3(x_0), \dots\}. \tag{1.2}$$

defined as the phase trajectory and originated from x_0.

1.1.3 Equilibrium Points

Definition 1.3. Consider x^* An equilibrium (or fixed) point of the system that satisfies

$$f(x^*) = x^*. \tag{1.3}$$

Remark. Graphically, equilibrium points are intersections of the curve $y = f(x)$, with the bisector $y = x$.

1.1.4 Periodic Orbits of Order p (p-Cycles)

Definition 1.4. [10] A point $x \in X$ is a periodic orbit of period p if

$$f^p(x) = x, \tag{1.4}$$

where p is the smallest positive integer satisfying this condition.
The set

$$\{x, f(x), f^2(x), \ldots, f^{p-1}(x)\} \tag{1.5}$$

which forms a p-cycle.

Remark. Periodic orbits are fundamental in bifurcations and the transition to chaos.

1.1.5 Phase Space

Definition 1.5. Consider a discrete dynamical system $f : X \to X$, where the set $X \subseteq \mathbb{R}^d$ represents the phase space, and each point $x \in X$ represents the system's complete state. The evolution of the system is described by the orbit

$$\mathcal{O}(x_0) = \{x_n\}_{n\in\mathbb{N}}, \quad x_{n+1} = f(x_n), \quad x_0 \in X. \tag{1.6}$$

Remark. The phase space encodes all possible orbits under the iteration of f, including fixed points, periodic orbits, and a periodic (chaotic) trajectories.

1.2 Stability

This section addresses the stability properties of equilibrium points in discrete systems. It includes formal criteria for Lyapunov and asymptotic stability, linearization techniques via the Jacobian matrix, and the use of Lyapunov functions for nonlinear stability analysis. These tools are critical for assessing the robustness of system trajectories under perturbations and form the basis for detecting bifurcations and chaotic behavior.

1.2.1 Lyapunov Stability and Asymptotic Stability

Definition 1.6. Let $f\colon X \to X$ be a map on the metric space (X, d), and let $x^* \in X$ satisfy $f(x^*) = x^*$.

1. **Lyapunov stability:**

$$\forall\, \varepsilon > 0\ \exists\, \delta > 0 :\ d(x_0, x^*) < \delta \implies d\big(f^n(x_0), x^*\big) < \varepsilon \quad \forall\, n \geq 0.$$

2. **Asymptotic stability:** x^* is Lyapunov stable and

$$\exists\, \delta' > 0 :\ d(x_0, x^*) < \delta' \implies \lim_{n\to\infty} f^n(x_0) = x^*.$$

1.2.2 Linearization

Definition 1.7. Let $f\colon U \subset \mathbb{R}^n \to \mathbb{R}^n$ be C^1 on an open U, and let $x^* \in U$ satisfy $f(x^*) = x^*$.

$$Df(x^*) \;=\; \Big[\partial_j f_i(x^*)\Big]_{1\leq i,j\leq n}$$

is the linearization of f at x^*.

Theorem 1.1 (**Hartman–Grobman**). *[14] Let $f\colon U \to \mathbb{R}^n$ be C^1 with fixed point x^*. If $Df(x^*)$ is hyperbolic (no eigenvalue on the unit circle), then there exist neighborhoods $V \ni x^*$, $W \ni 0$ and a homeomorphism $h\colon V \to W$ such that*

$$h\big(f(x)\big) \;=\; Df(x^*)\, h(x) \quad \forall\, x \in V.$$

1.2.3 Nature of Equilibrium via Linearization

Let $f\colon U \subset \mathbb{R}^n \to \mathbb{R}^n$ be C^1 and $x^* \in U$ a fixed point, $f(x^*) = x^*$. Denote $A = Df(x^*)$ and let its eigenvalues be $\{\lambda_i\}_{i=1}^n$. Then the linearized map $x_{k+1} = A\, x_k$ determines the local behavior of the nonlinear system:

- **Hyperbolic Sink (Asymptotically Stable):** $\forall i,\ |\lambda_i| < 1$. All trajectories in a neighborhood converge exponentially to x^*.
- **Hyperbolic Source (Unstable):** $\forall i,\ |\lambda_i| > 1$. All nearby trajectories diverge exponentially from x^*.
- **Hyperbolic Saddle:** $\exists\, i, j$ such that $|\lambda_i| < 1$ and $|\lambda_j| > 1$. Trajectories approach x^* along the stable eigenspace and diverge along the unstable one.
- **Non-Hyperbolic (Center or Indeterminate):** $\exists i$ with $|\lambda_i| = 1$. Linearization is inconclusive; higher-order terms or Lyapunov functions are required.

1.2.4 Lyapunov Function

Theorem 1.2. *[16] Let U be a neighborhood of the equilibrium x^*.*
$V : U \to \mathbb{R}$ is a Lyapunov function that satisfies:

1. **Positivity:** $V(x^*) = 0$ and $V(x) > 0$ for all $x \in U \setminus \{x^*\}$.
2. **Non-Increase Along Orbits:**

$$V(f(x)) - V(x) \leq 0 \quad \text{for all } x \in U. \tag{1.7}$$

If

$$V(f(x)) - V(x) < 0 \quad \text{for all } x \in U \setminus \{x^*\}, \tag{1.8}$$

then x^* is asymptotically stable.

Theorem 1.3 (**Discrete-Time Lyapunov Stability**)**.** *[16] Consider a discrete system $x_{k+1} = Ax_k$, where $A \in \mathbb{R}^{n\times n}$. The system is globally asymptotically stable if and only if, for any positive definite matrix $Q \in \mathbb{R}^{n\times n}$, there exists a unique positive definite matrix $P \in \mathbb{R}^{n\times n}$ satisfying the Lyapunov equation:*

$$A^T PA - P + Q = 0. \tag{1.9}$$

The quadratic function

$$V(x) = x^T Px \tag{1.10}$$

is a valid Lyapunov function, which proves the system's stability.

1.3 Bifurcation Theory in Discrete Systems

Bifurcation theory studies the changes in a dynamical system's behavior when certain adjustments are made to its parameters. In discrete systems specifically, bifurcations lead to the appearance or disappearance of fixed points or periodic orbits, resulting in the onset of chaos.

1.3.1 Definition of Bifurcation

Definition 1.8. [12] Consider the discrete dynamical system:

$$x_{k+1} = f(x_k, \lambda), \quad k \in \mathbb{N}, \tag{1.11}$$

where $x \in \mathbb{R}^n$ and $\lambda \in \mathbb{R}$ is a parameter.

A **bifurcation** happens at a critical parameter value λ^* if there is an adjustment in the structure of the fixed points or periodic orbits of f.

1.3.2 Role of Bifurcations in Chaos

Bifurcations are fundamental in the transition to chaos. For example, a cascade of **period-doubling** bifurcations lead to a chaotic regime, while **Neimark-Sacker** bifurcations introduce **quasiperiodic behavior** that results in complex, chaotic dynamics.

1.3.3 Fundamental Types of Bifurcations

Saddle-Node (Tangent) Bifurcation

Two fixed points (one stable, one unstable) merge and disappear. [12] For the normal form

$$x_{k+1} = x_k + \lambda - x_k^2, \tag{1.12}$$

the conditions are:

- **Existence:** $f(x^*, \lambda^*) = x^*$.
- **Tangency:** $\frac{\partial f}{\partial x}(x^*, \lambda^*) = 1$.
- **Non-degeneracy:** $\frac{\partial^2 f}{\partial x^2}(x^*, \lambda^*) \neq 0$.

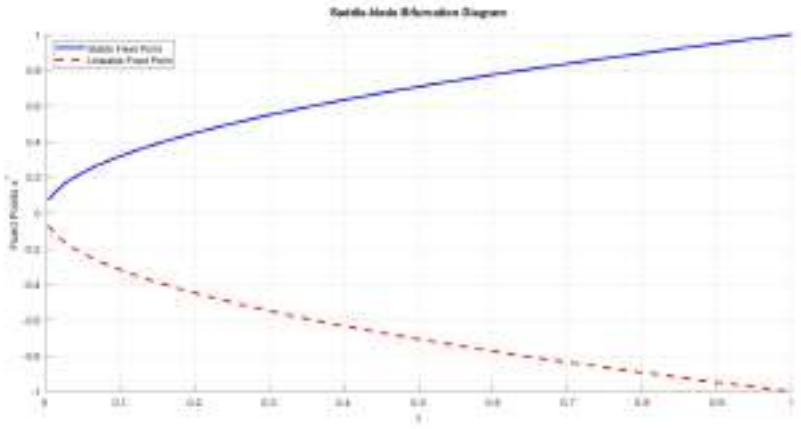


Figure 1.1: Saddle-Node Bifurcation Diagram

Transcritical Bifurcation

Two fixed points exchange stability. [12] The normal form is

$$x_{k+1} = x_k + \lambda x_k - x_k^2. \tag{1.13}$$

Here, fixed points exist at $x = 0$ and $x = \lambda$; as λ crosses zero, the stability properties of these fixed points are interchanged.

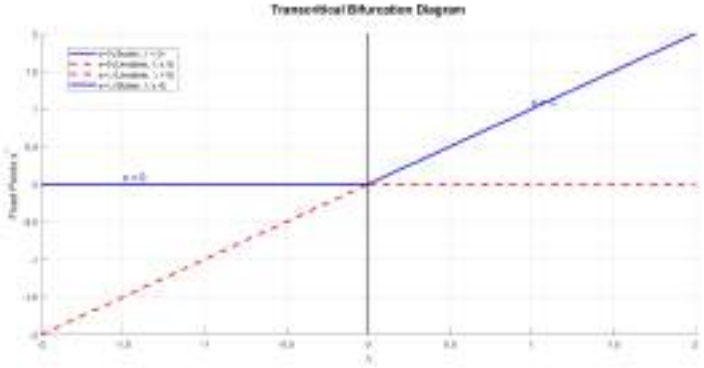


Figure 1.2: Transcritical Bifurcation Diagram

Pitchfork Bifurcation

A pitchfork bifurcation happens in systems with symmetry. [12] The normal form

$$x_{k+1} = x_k + \lambda x_k - x_k^3 \tag{1.14}$$

has these features:

- For $\lambda < 0$, the unique fixed point $x = 0$ is stable.
- For $\lambda > 0$, $x = 0$ becomes unstable and two new fixed points emerge at $x = \pm\sqrt{\lambda}$.

The bifurcation is termed **supercritical** if the new fixed points are stable, and **subcritical** if they are unstable.

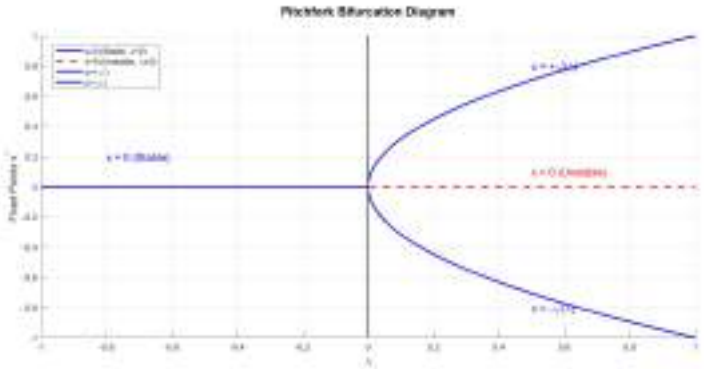


Figure 1.3: Pitchfork Bifurcation Diagram

1.3.4 Bifurcations Leading to Chaos

Period-Doubling Bifurcation

A period-doubling bifurcation happens when a fixed point (or periodic orbit) loses stability as an eigenvalue crosses -1, leading to a new orbit with twice the period. [12] For example, in the logistic map

$$x_{k+1} = \lambda x_k(1 - x_k), \tag{1.15}$$

this happens when

$$f'(x^*, \lambda^*) = -1. \tag{1.16}$$

Remark. Successive period-doubling bifurcations can form a cascade that leads to chaos.

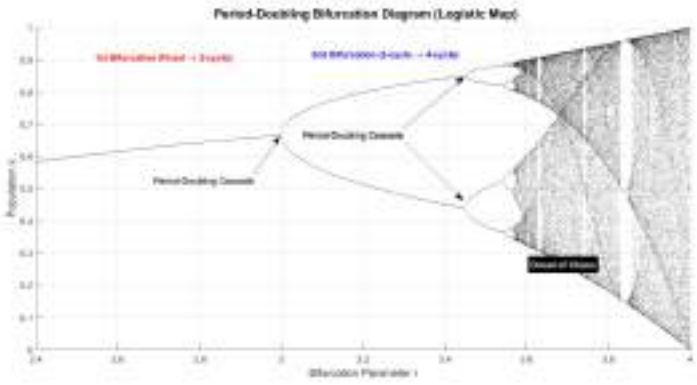


Figure 1.4: Period-Doubling Bifurcation Diagram

Neimark-Sacker Bifurcation

The Neimark-Sacker bifurcation happens when a pair of complex conjugate eigenvalues of $Df(x^*, \lambda)$ cross the unit circle (with $|\mu| = 1$ and $\mu \neq \pm 1$). This transition gives rise to an invariant closed curve and quasiperiodic dynamics. [2]

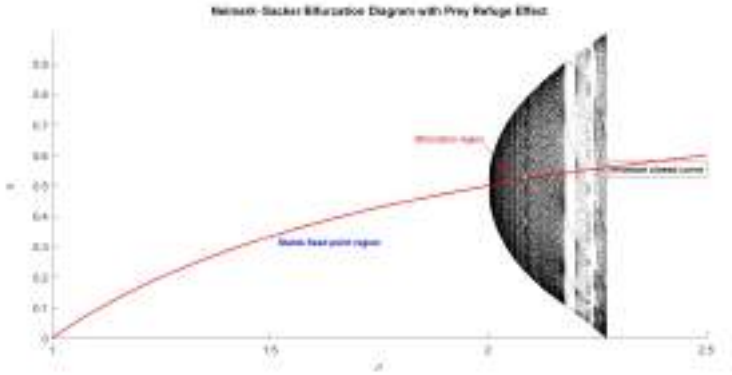


Figure 1.5: Neimark-Sacker Bifurcation Diagram with Prey Refuge Effect

Crisis Bifurcation

A crisis bifurcation is a sudden change in the size or shape of a chaotic attractor as the parameter λ varies. It happens when the attractor collides with an unstable periodic orbit, causing a sudden chaos appearance or disappearance. [2]

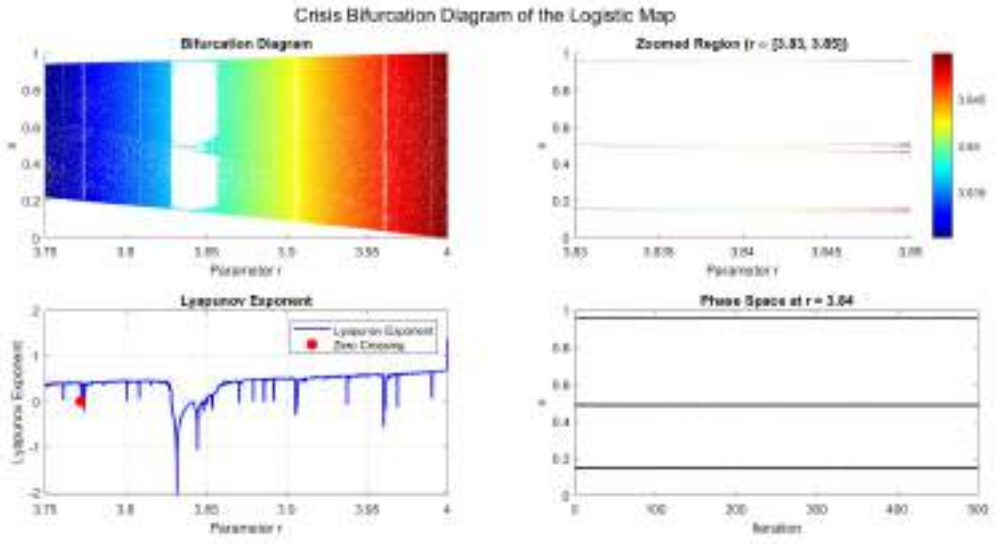


Figure 1.6: Crisis Bifurcation Diagram

1.3.5 Special Case in Non-Smooth Systems

Border-Collision Bifurcation [32] [5]

Consider a family of maps

$$x_{n+1} = \begin{cases} f_L(x, \mu), & \text{if } h(x) \leq 0, \\ f_R(x, \mu), & \text{if } h(x) \geq 0, \end{cases}$$

where $x \in \mathbb{R}^n$, $\mu \in \mathbb{R}$, and f_L, f_R are smooth. The border is defined by

$$\Sigma = \{x \in \mathbb{R}^n : h(x) = 0\}.$$

A border-collision bifurcation happens at $\mu = \mu_c$ when an invariant set satisfies $h(x^*) = 0$, causing the orbit to lie on the border Σ. At this point, the Jacobian changes discontinuously, and the system's dynamics change suddenly as μ crosses μ_c.

For example, a one-dimensional normal form :

$$x_{n+1} = \begin{cases} \mu + A_L\, x_n, & x_n \leq 0, \\ \mu + A_R\, x_n, & x_n \geq 0, \end{cases}$$

where the fixed point is at $x^* = 0$ when $\mu = 0$ and the bifurcation happens as μ passes through zero.

Remark. Although the map is continuous at $x = 0$, the derivative jumps from A_L to A_R.

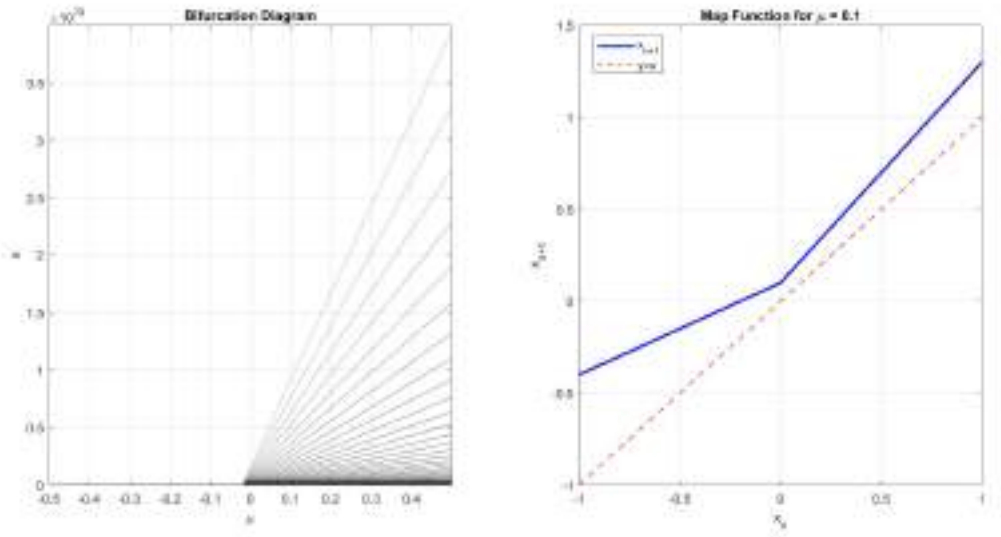


Figure 1.7: Border-Collision Bifurcation and its Map Function Plots.

Bifurcation Diagram (Left Plot):

- **X-axis:** Parameter μ
- **Y-axis:** Asymptotic values of x after transients
- **Purpose:** Displays the long-term attractor for each μ and highlights the border collision at $\mu = 0$ where the fixed point $x^* = 0$ changes behavior due to the derivative jump.

Map Function Plot (Right Plot):

- **X-axis:** Current state x_n
- **Y-axis:** Next state x_{n+1} for a fixed μ (e.g., $\mu = 0.1$)
- **Purpose:** Shows the piecewise linear map. The blue curve is the function x_{n+1}, and the red dashed line is $y = x$; their intersection indicates the fixed point, with the slope change at $x = 0$ illustrating the border collision.

1.4 Summary

In this chapter, we reviewed some of the basic concepts of discrete dynamical systems and their behavior, and this helped us analyze these systems. These ideas pave the way for the next chapter, where we explore comprehensive chaotic discrete dynamical systems, their mathematical properties, and their role in chaos theory.

Chapter 2

Chaos Quantification Tools

2.1 Chaos in Discrete Systems

This chapter presents rigorous tools for identifying and quantifying chaos in discrete dynamical systems. It introduces Devaney's definition of chaos and formalizes sensitivity to initial conditions using Lyapunov exponents. It further explores Feigenbaum's universal constants in period-doubling cascades and the use of fractal dimensions to characterize strange attractors. These tools form the analytical foundation for studying chaotic behavior in discrete maps.

Definition 2.1. A system is chaotic if small changes in the initial conditions lead to very different outcomes. This makes the system unpredictable over time, even though it follows fixed rules.

Definition 2.2. [4] A discrete dynamical system is **chaotic** (in the sense of Devaney) if the map $f : X \to X$ satisfies the following three conditions:

1. **Sensitivity to Initial Conditions:**
   There exists a constant $\delta > 0$ such that for any point $x_0 \in X$ and any neighborhood U of x_0, there exists a point $y_0 \in U$ and an integer $n \geq 0$ such that
   $$|f^n(x_0) - f^n(y_0)| > \delta. \tag{2.1}$$

2. **Topological Mixing:**
   For any two non-empty open sets $U, V \subset X$, there exists an integer $N > 0$ such that for all $n \geq N$,
   $$f^n(U) \cap V \neq \emptyset. \tag{2.2}$$

3. **Density of Periodic Orbits:**
   The set of periodic points of f is dense in X. That is, for every point $x \in X$ and every neighborhood U of x, there exists a periodic point $p \in U$ such that
   $$f^k(p) = p \quad \text{for some } k \in \mathbb{N}. \tag{2.3}$$

2.1.1 Lyapunov Exponents: Measuring Sensitivity to Initial Conditions

Definition 2.3 (Lyapunov Exponent)**.** [6] Let $f : \mathbb{R} \to \mathbb{R}$ be a differentiable map defining the discrete dynamical system

$$x_{n+1} = f(x_n), \tag{2.4}$$

and let $x_0 \in \mathbb{R}$ be an initial condition. The *Lyapunov exponent* at x_0, denoted $\lambda(x_0)$, is defined as

$$\lambda(x_0) = \lim_{n\to\infty} \frac{1}{n} \sum_{k=0}^{n-1} \ln |f'(x_k)|, \tag{2.5}$$

provided the limit exists, where $x_k = f^k(x_0)$ denotes the k-th iterate of the initial condition.

Theorem 2.1 (Lyapunov Exponents and Stability in Discrete Dynamical Systems)**.** *[6] Let $f : \mathbb{R} \to \mathbb{R}$ be a differentiable map defining a discrete dynamical system*

$$x_{n+1} = f(x_n), \tag{2.6}$$

and let $x_0 \in \mathbb{R}$ be an initial condition. Suppose the orbit $\{x_n\}$ remains in a compact set and that the derivative $f'(x)$ exists and is continuous. Then the Lyapunov exponent is given by

$$\lambda(x_0) = \lim_{n\to\infty} \frac{1}{n} \sum_{k=0}^{n-1} \ln |f'(x_k)|, \tag{2.7}$$

provided the limit exists. Then:

- *If $\lambda(x_0) < 0$, the orbit is* asymptotically stable *near x_0.*
- *If $\lambda(x_0) > 0$, the orbit exhibits* chaotic behavior *near x_0 (sensitive dependence on initial conditions).*
- *If $\lambda(x_0) = 0$, the system is at a* bifurcation point *(neither converging nor diverging exponentially).*

Proof. [6] Let the orbit be defined by

$$x_n = f^n(x_0), \tag{2.8}$$

and consider a small perturbation δ_0 of the initial condition, so that the perturbed orbit begins at $x_0 + \delta_0$. Let δ_n denote the deviation from the reference orbit after n iterations. Linearizing the map gives

$$\delta_{n+1} \approx f'(x_n)\, \delta_n. \tag{2.9}$$

By iterating this relation, we get

$$\delta_n \approx \delta_0 \prod_{k=0}^{n-1} f'(x_k). \tag{2.10}$$

Taking logarithms of the absolute value on both sides:

$$\ln|\delta_n| \approx \ln|\delta_0| + \sum_{k=0}^{n-1} \ln|f'(x_k)|\,. \tag{2.11}$$

Dividing both sides by n gives:

$$\frac{1}{n}\ln|\delta_n| \approx \frac{1}{n}\ln|\delta_0| + \frac{1}{n}\sum_{k=0}^{n-1} \ln|f'(x_k)|\,. \tag{2.12}$$

Taking the limit as $n \to \infty$, and noting that $\frac{1}{n}\ln|\delta_0| \to 0$, we conclude:

$$\lim_{n\to\infty} \frac{1}{n}\ln|\delta_n| = \lambda(x_0). \tag{2.13}$$

Thus, the sign of $\lambda(x_0)$ determines whether small deviations from the reference orbit grow or decay exponentially, indicating local instability (chaos) or stability near x_0. □

Dynamical Regime	**Lyapunov Exponent Spectrum**	**Characteristic**
Fixed Point	All $\lambda_i < 0$	Exponential convergence to a single equilibrium.
Periodic Orbit	One $\lambda_1 = 0$, all others $\lambda_{i>1} < 0$	Neutral direction along the cycle; contraction transverse to it.
Quasi-Periodic	k exponents $\lambda_{1\ldots k} = 0$, rest < 0	Invariant k-torus; motion with k incommensurate frequencies.
Chaotic	Exactly one $\lambda_1 > 0$, all others $\lambda_{i>1} \leq 0$	Sensitive dependence on initial conditions; strange attractor of fractal geometry.
Hyperchaotic	At least two $\lambda_1, \lambda_2 > 0$, rest ≤ 0	Two (or more) expanding directions; more complex attractor with higher information dimension.

Table 2.1: Lyapunov exponent conditions and their corresponding dynamical regimes.

2.1.2 Feigenbaum's Constants

Feigenbaum's constants describe the period-doubling route to chaos in discrete dynamical systems.

1. **Feigenbaum constant (δ):**
   $\delta \approx 4.6692$ is the ratio of the distances between successive bifurcations in the period-doubling route. It is universal for systems exhibiting this route:

$$\lim_{n\to\infty} \frac{x_{n+1} - x_n}{x_n - x_{n-1}} = \delta \approx 4.6692.$$

2. **Feigenbaum constant (α):**
   $\alpha \approx 2.5029$ is the ratio of the widths of the bifurcation intervals, also universal:

$$\lim_{n\to\infty} \frac{I_{n+1}}{I_n} = \alpha \approx 2.5029.$$

- **Universality:** These constants apply to all systems with period-doubling bifurcations, such as the logistic map.
- **Chaos theory:** They quantify the transition from periodic behavior to chaos.

2.1.3 Fractal Dimensions and Strange Attractors in Discrete Maps

- **Strange attractors** in discrete maps are invariant chaotic sets characterized by non-integer fractal dimensions. These dimensions (eg., the box-counting dimension) quantify the complexity and scale invariance of the attractor.

  Definition 2.4. [32] Let $f : \mathbb{R}^n \to \mathbb{R}^n$ be a discrete map, and let $A \subset \mathbb{R}^n$ be a chaotic attractor. Then the box-counting dimension $\dim_B(A)$ satisfies

  $$\dim_B(A) < n, \quad \text{with} \quad \dim_B(A) \notin \mathbb{Z}, \tag{2.14}$$

  where $\dim_B(A)$ denotes the box-counting dimension of the set A.

- **Fractal dimensions** are also related to Lyapunov exponents through the Kaplan–Yorke conjecture.

  Definition 2.5. [32] Let $\{\lambda_i\}$ denote the Lyapunov exponents ordered as $\lambda_1 \geq \lambda_2 \geq \cdots$, and let j be the largest index such that

  $$\sum_{i=1}^{j} \lambda_i \geq 0. \tag{2.15}$$

  Then the Kaplan–Yorke dimension is defined by

  $$D_{KY} = j + \frac{\sum_{i=1}^{j} \lambda_i}{|\lambda_{j+1}|}. \tag{2.16}$$

2.2 Summary

This chapter introduced the chaos tools. We discussed the definition of chaos, including sensitivity to initial conditions, topological mixing, and the density of periodic orbits. Lyapunov exponents were presented for measuring sensitivity, and their role in stability was clarified through the associated theorem. Feigenbaum's constants were highlighted, emphasizing their universality in period-doubling bifurcations. Additionally, we examined fractal dimensions and strange attractors, linking them to Lyapunov exponents via the Kaplan–Yorke conjecture.

Chapter 3

Key Discrete Chaotic Maps

This chapter examines fundamental discrete-time chaotic maps that serve as canonical models in chaos theory. These include the Logistic, Hénon, Lozi, and discrete Lorenz maps. Each system is analyzed through its defining equations, attractor geometry, bifurcation structure, and Lyapunov exponent evolution to highlight the onset and development of chaos in low-dimensional dynamics.

3.1 Logistic Map

The *Logistic map* is a discrete dynamical system, defined by :

$$x_{n+1} = r x_n (1 - x_n) \tag{3.1}$$

where:

- x_n is the state variable at time step n,
- r is a real parameter that influences the system's behavior.

Strange Attractor Plot

The figure below presents the scatter plot of the Logistic map's strange attractor for the parameter value: $r = 3.9$

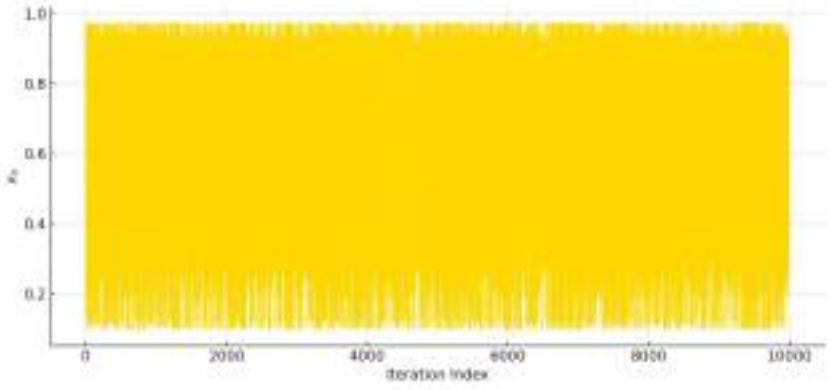


Figure 3.1: Logistic Map Attractor for $r = 3.9$.

The first 1,000 iterates are discarded as transients, and the subsequent 100,000 points are also plotted to show the strange attractor.

Remark. The logistic map is a 1D discrete nonlinear map, it does have a strange attractor, but it doesn't have a visible geometric structure in phase space like the Hénon, Lozi or Lorenz attractors. It lacks the complex geometry in 2D maps because the entire trajectory lies on a line, not a plane.

First 100 Iterations

The time series plot below shows the evolution of x_n over the first 100 iterations, starting from: $x_0 = 0.4$
The resulting sequence displays irregular, non-repeating fluctuations indicative of chaotic behavior.

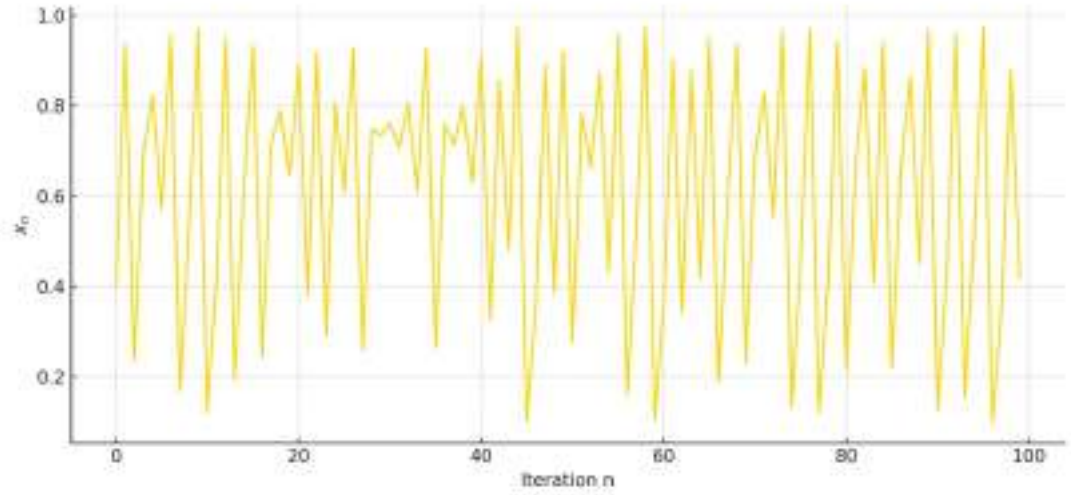


Figure 3.2: Logistic Map – First 100 Iterations of x_n

Bifurcation Diagram

By varying the parameter r from 2.5 to 4.0 and fixing the initial condition: $x_0 = 0.4$ we obtain the bifurcation diagram by discarding the first 1,000 transient values and plotting the next 100 iterates of x_n for each r. This diagram demonstrates the period-doubling route to chaos.

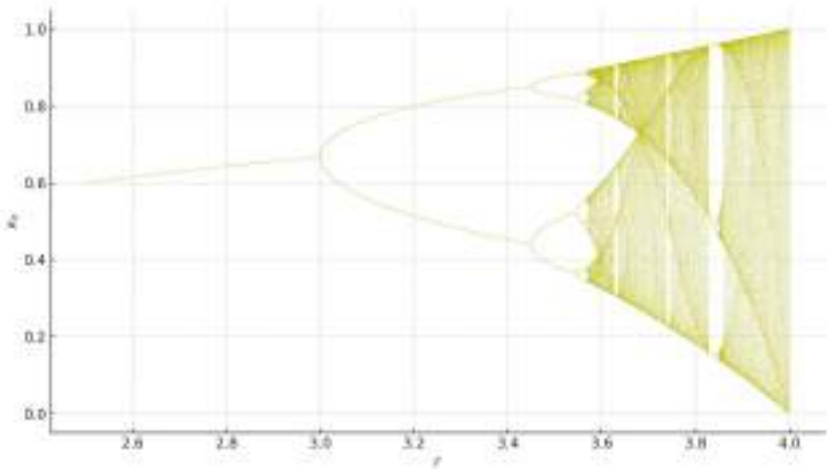


Figure 3.3: Logistic Map Bifurcation Diagram for $x_0 = 0.4$

The Lyapunov exponent evolution

This visualization shows how the Lyapunov exponent changes as parameter r varies from 2.5 to 4.0. Note the transition to positive values (above the gray line) marking the onset of chaos, and the complex structure with periodic windows where the exponent dips below zero.

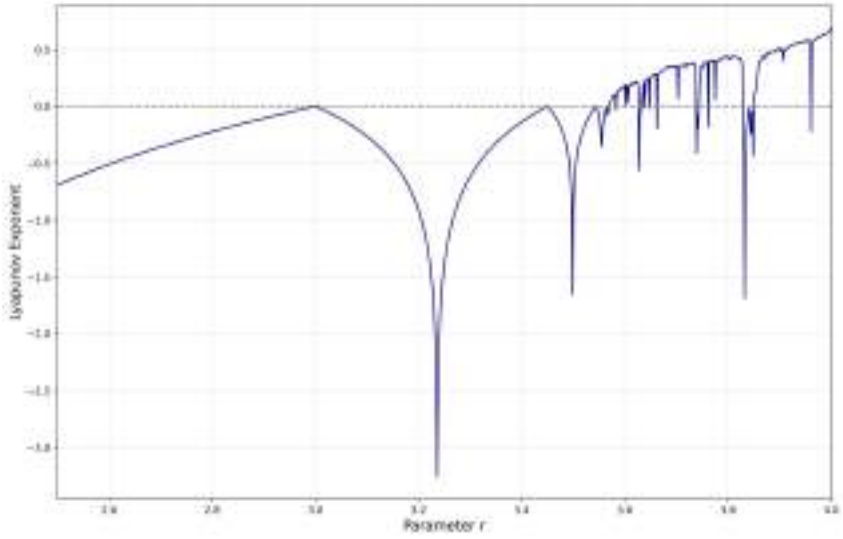


Figure 3.4: Logistic Map : Lyapunov Exponent Evolution

3.2 Hénon Map

Definition 3.1. [29] The *Hénon map* is a discrete-time dynamical system defined by:

$$\begin{cases} x_{n+1} &= 1 - a\,x_n^2 + y_n, \\ y_{n+1} &= b\,x_n, \end{cases} \tag{3.2}$$

where a and b are real parameters.

Strange Attractor Plot

The figure below presents the scatter plot of the Hénon attractor for

$$a = 1.7, \quad b = 0.5.$$

The initial 1 000 iterates were discarded as transients, and the next 100 000 points were plotted:

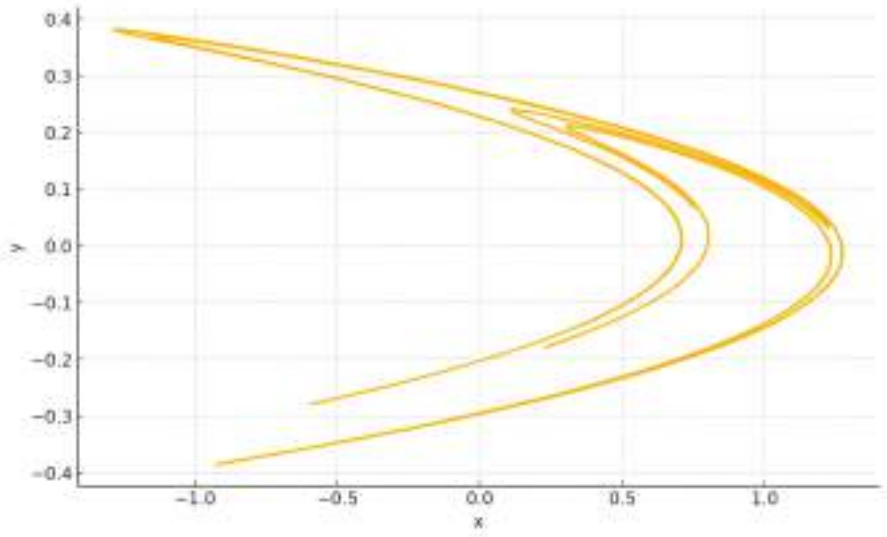


Figure 3.5: Hénon Strange Attractor for $a = 1.4$, $b = 0.3$.

First 100 Iterations

The time series of x_n over the first 100 iterations, starting from $(x_0, y_0) = (0, 0)$, reveals a non-repeating, irregular fluctuation indicative of chaotic dynamics:

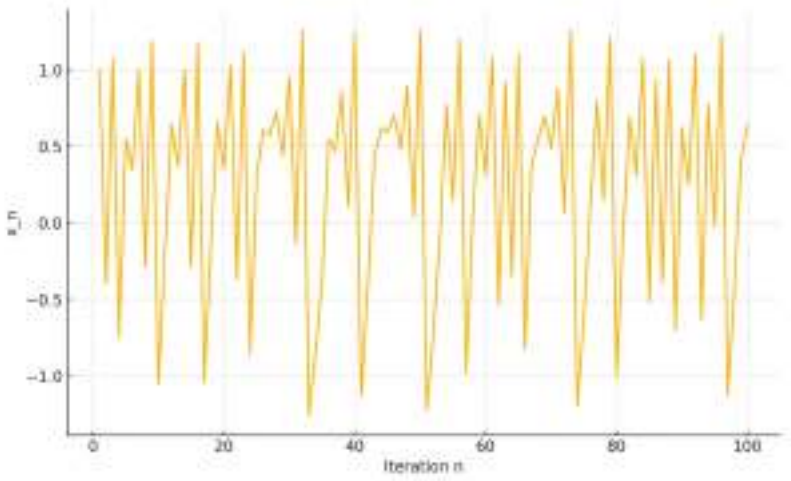


Figure 3.6: Hénon Map – First 100 Iterations of x_n

Bifurcation Diagram

Varying the parameter a from 0.5 to 1.4, while fixing $b = 0.3$, and discarding the first 1 000 transient points for each value of a, we obtain the orbit diagram (also known as a bifurcation diagram) by plotting the next 100 values of x_n. This visualization illustrates the period-doubling route to chaos:

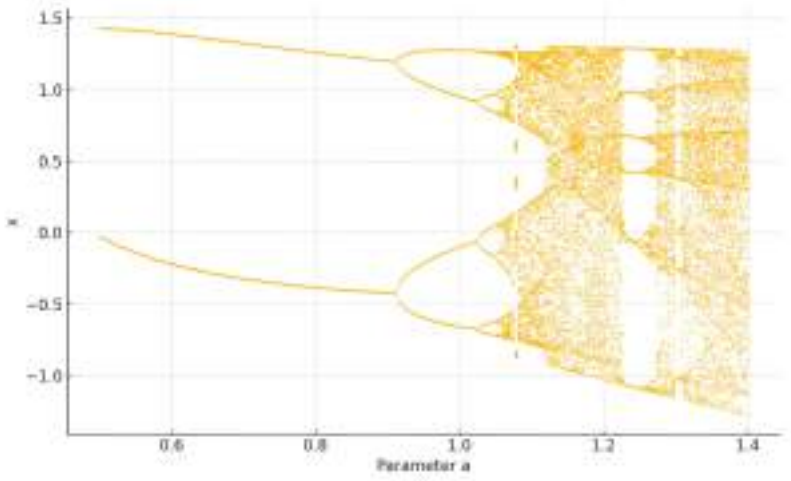


Figure 3.7: Hénon Map Bifurcation Diagram for $b = 0.3$.

The Lyapunov exponent evolution

For the Hénon map, we can see the evolution of the Lyapunov exponent as parameter a varies from 0.5 to 1.4 with fixed $b = 0.3$. The system transitions to chaos when the exponent becomes positive.

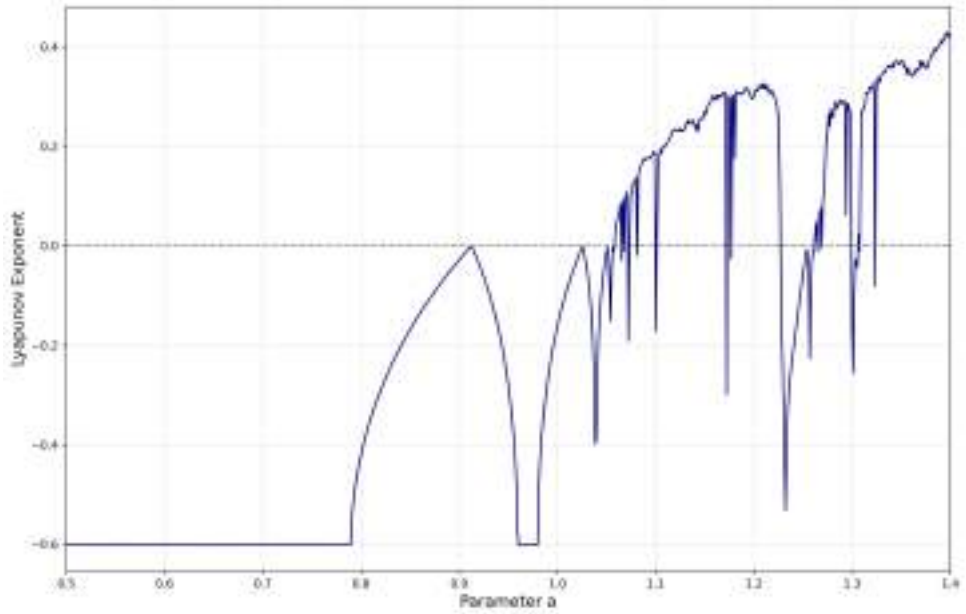


Figure 3.8: Hénon Map : Lyapunov Exponent Evolution

3.3 Lozi Map

Definition 3.2. [18] The *Lozi map* is a two-dimensional discrete-time dynamical system defined by:

$$\begin{cases} x_{n+1} = 1 - a\,|x_n| + y_n, \\ y_{n+1} = b\,x_n, \end{cases} \tag{3.3}$$

where $a, b \in \mathbb{R}$. This map was introduced by R. Lozi as a piecewise-linear simplification of the *Hénon map*.

Strange Attractor Plot

The long-term behavior of the system reveals a fractal geometric structure known as the *Lozi attractor*. The figure below shows a scatter plot of the trajectory (x_n, y_n) with parameters

$$a = 1.7, \quad b = 0.5.$$

The first 1 000 iterates are discarded as transients, and the following 100 000 points are plotted:

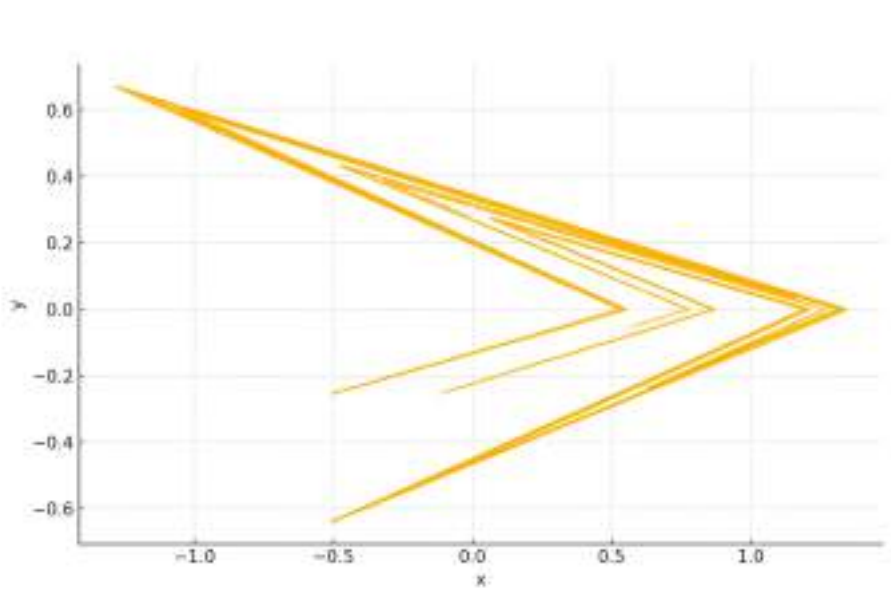


Figure 3.9: Lozi Strange Attractor for $a = 1.7$, $b = 0.5$.

First 100 Iterations

Starting from the initial condition $(x_0, y_0) = (0, 0)$, the time series of x_n for the first 100 iterations exhibits irregular and non-periodic fluctuations, indicating the presence of chaotic dynamics:

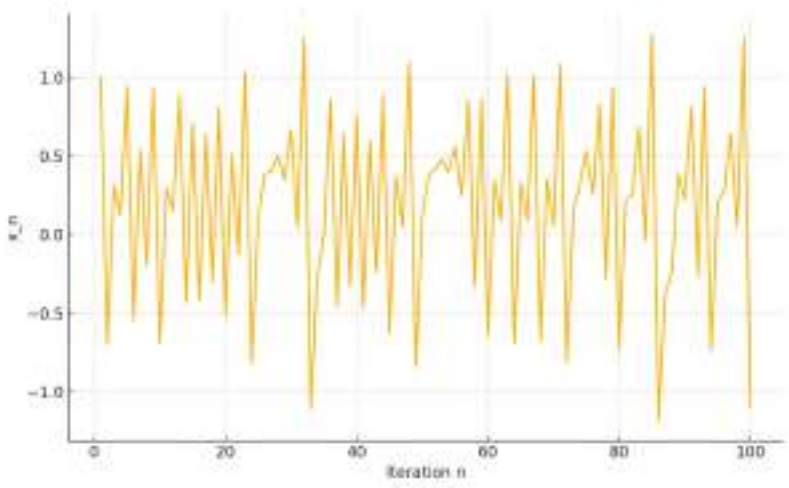


Figure 3.10: Lozi Map – First 100 Iterations of x_n.

Bifurcation Diagram

To visualize the onset of chaos, we vary the parameter $a \in [0.5, 2.0]$ while keeping $b = 0.5$ fixed. For each value of a, the initial 1 000 iterates are discarded to remove transient effects, and the next 100 iterates of x_n are plotted. The resulting diagram exhibits a period-doubling cascade interspersed with periodic windows:

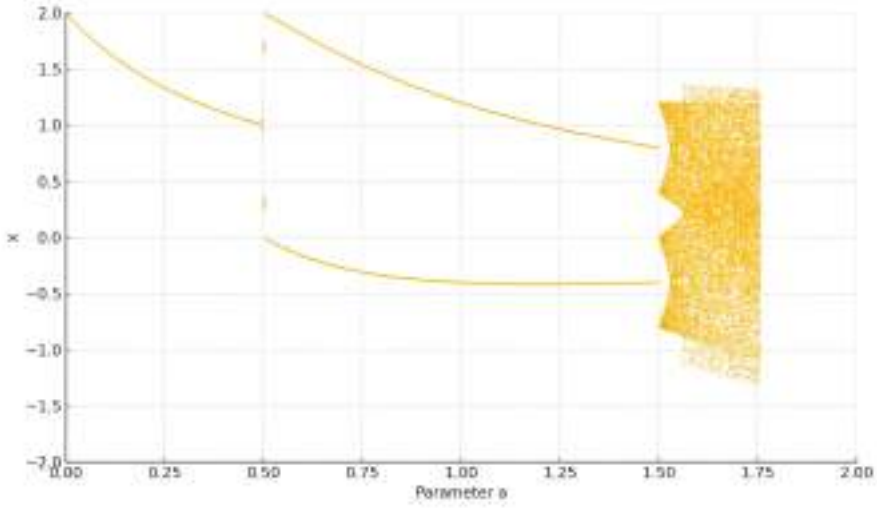


Figure 3.11: Lozi Map Bifurcation Diagram for $b = 0.5$.

The Lyapunov exponent evolution

This shows the Lyapunov exponent of the Lozi map as parameter a varies from 0.5 to 1.7 with fixed $b = 0.5$. Note the distinct transition points and regions of chaos.

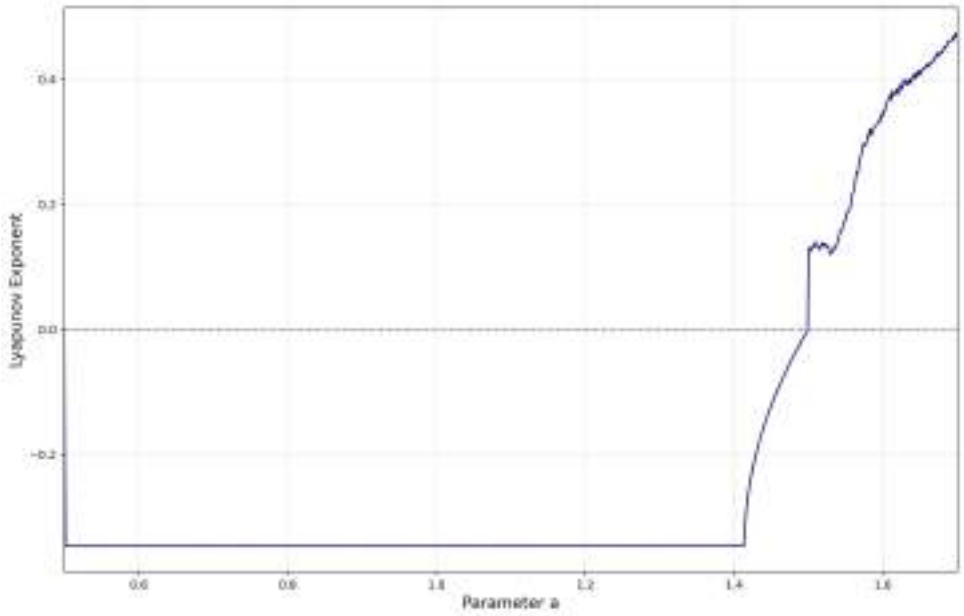


Figure 3.12: Lozi Map : Lyapunov Exponent Evolution

3.4 Lorenz Map

Definition 3.3. [33] The discrete *Lorenz map* is defined by the following system of equations:

$$\begin{cases} x_{k+1} &= (1 + a\,b)\,x_k - b\,y_k\,x_k, \\ y_{k+1} &= (1 - b)\,y_k + b\,x_k^2, \end{cases} \tag{3.4}$$

where a and b are real parameters.

Strange Attractor Plot

The plot below shows the long-term scatter of the points (x_n, y_n) after discarding the first 1,000 transient iterations and plotting the subsequent 100,000 points. The attractor for

$$a = 1.25, \quad b = 0.75, \tag{3.5}$$

displays complex, fractal behavior, characteristic of chaotic systems:

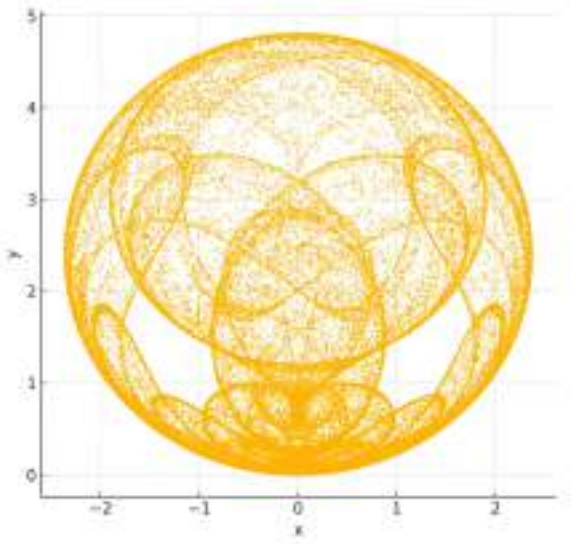


Figure 3.13: Lorenz Strange Attractor for $a = 1.25$, $b = 0.75$.

First 100 Iterations

Starting from the initial condition $(x_0, y_0) = (0.1, 0.1)$, the first 100 values of x_n exhibit irregular and non-periodic fluctuations, a clear indication of chaotic dynamics. This irregularity demonstrates the sensitive dependence on initial conditions, a hallmark of chaos:

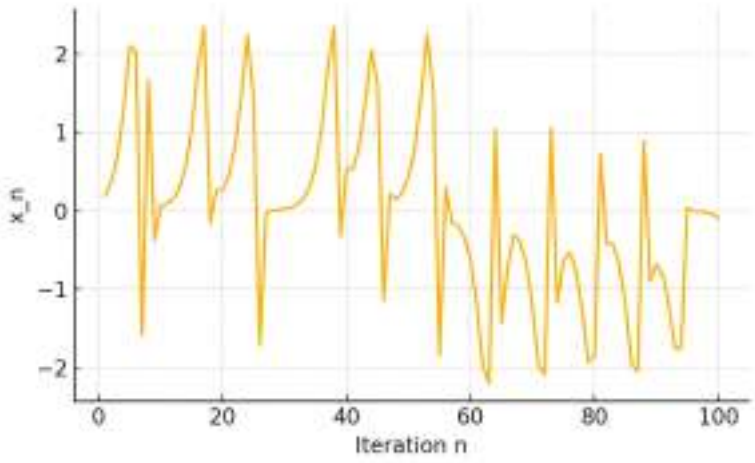


Figure 3.14: Lorenz Map – First 100 Iterations of x_n.

Bifurcation Diagram

To explore the bifurcation behavior, we vary the parameter a from 0.0 to 2.0, keeping $b = 0.75$. The first 500 transient iterations are discarded, and the subsequent 200 iterations of x_n are plotted. The resulting bifurcation diagram reveals a period-doubling cascade starting around $a \approx 0.8$, progressing to chaotic regimes that persist up to $a = 2.0$:

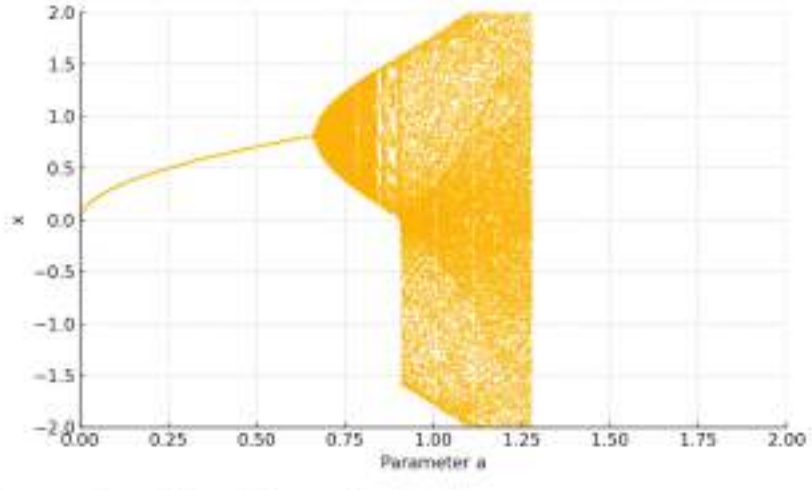


Figure 3.15: Lorenz Map Bifurcation Diagram for $a \in [0, 2]$, $b = 0.75$.

The Lyapunov exponent evolution

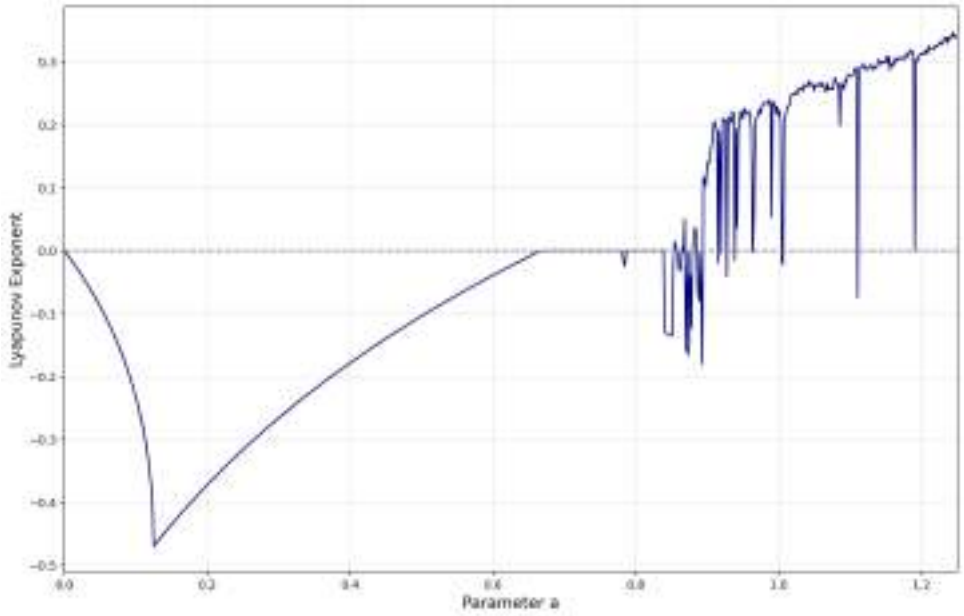


Figure 3.16: Lorenz Map : Lyapunov Exponent Evolution

For the Lorenz map, this visualization shows how the Lyapunov exponent evolves as parameter a varies from 0.0 to 1.25 with fixed $b = 0.75$.

3.5 Summary

In this chapter, we explored the key discrete chaotic maps, focusing on their chaotic behavior. such as the logistic, Hénon, Lozi, and Lorenz maps, and illustrated the onset of chaos and its fractal structure through bifurcation and attractor plots, and the evolution of Lyapunov exponents diagrams.

Chapter 4

Synchronization of Chaos in Discrete Dynamical Systems

This chapter develops the theory and methods for synchronizing chaotic behavior in discrete-time systems. It begins by formalizing the concept of chaos synchronization and its mathematical definition for master–slave configurations. We then classify synchronization regimes—complete, anti-, phase, lag, generalized, projective, hybrid and Q–S—and present the corresponding existence theorems based on conditional Lyapunov exponents or contraction mappings. Finally, we review principal design techniques (active and adaptive control) for enforcing synchronization, illustrated by representative examples.

4.1 The Concept of Chaos Synchronization

The origin of the word *synchronization* is a Greek root συν (*syn*) and χρόνος (*chronos*), which means "to share the common time".
The original meaning of *synchronization* has been maintained up to now in the colloquial use of this word, as agreement or correlation in time of different processes. [25]

4.2 Definition and Importance of Synchronization

Definition 4.1. [25] **Synchronization of chaos** refers to the process by which two (or more) chaotic systems—either identical or different—adjust a property of their motion to behave similarly due to coupling or external forcing (periodic or noisy).

Definition 4.2. [25] **Synchronization of chaotic systems** refers to the alignment of the trajectories of coupled chaotic systems, despite their inherent sensitivity to initial conditions.

Definition 4.3. [25] **Synchronization of Discrete Systems**
Consider two discrete dynamical systems, a drive (master) system

$$x_{n+1} = f(x_n), \tag{4.1}$$

and a response (slave) system

$$y_{n+1} = g(y_n) + u_n, \tag{4.2}$$

with control input u_n. The systems are said to be *synchronized* if

$$\lim_{n\to\infty} \|y_n - x_n\| \to 0 \tag{4.3}$$

Remark. The importance of chaos synchronization spans multiple disciplines:

- **Secure Communications**: Synchronized chaotic systems are used to mask, transmit, and recover information securely.
- **Control Engineering**: Synchronization provides insights into controlling highly nonlinear systems.
- **Neural Networks**: Synchronization models the coordination of neural activity in the brain.
- **Biological Systems**: Many biological processes, such as heart rhythm and circadian cycles, exhibit synchronized chaotic behavior.
- **Physics**: Synchronization helps explain phenomena like coherence in laser systems and superconducting Josephson junctions.

4.3 Types of Synchronization

4.3.1 Complete Synchronization

Definition 4.4. [12] Two chaotic systems

$$X(k+1) = F(X(k)) \quad \text{and} \quad Y(k+1) = G(Y(k)) + U \tag{4.4}$$

(with $F = G$) achieve complete synchronization when:

$$\lim_{k\to\infty} \|Y(k) - X(k)\| = 0 \tag{4.5}$$

Theorem 4.1 (**Complete Synchronization Theorem**). *[25] Let $\mathcal{M}$ and $\mathcal{S}$ be two coupled chaotic systems described by*

$$X(k+1) = F(X(k)), \quad Y(k+1) = G(Y(k)) + U \tag{4.6}$$

where $F = G$ and U is a coupling function. If there exists a coupling scheme such that all conditional Lyapunov exponents of the variational equation for the error dynamics are negative, then the systems achieve complete synchronization:

$$\lim_{k\to\infty} \|Y(k) - X(k)\| = 0. \tag{4.7}$$

Proof. Define the synchronization error:

$$e(k) = Y(k) - X(k). \tag{4.8}$$

The error dynamics evolve as:

$$e(k+1) = F(Y(k)) - F(X(k)) + U. \tag{4.9}$$

By the mean value theorem, there exists $Z(k) \in [X(k), Y(k)]$ such that:

$$F(Y(k)) - F(X(k)) = DF(Z(k)) \cdot e(k), \tag{4.10}$$

where $DF(Z(k))$ is the Jacobian of F at $Z(k)$. Using coupling $U = -Ke(k)$, the error becomes:

$$e(k+1) = [DF(Z(k)) - K] \cdot e(k). \tag{4.11}$$

Complete synchronization occurs when all eigenvalues of $[DF(Z(k)) - K]$ have moduli less than one, i.e., when all conditional Lyapunov exponents

$$\lambda_i = \lim_{n\to\infty} \frac{1}{n} \sum_{k=0}^{n-1} \ln |\mu_i(k)| < 0 \quad \forall i, \tag{4.12}$$

where $\mu_i(k)$ are eigenvalues of $[DF(Z(k)) - K]$. Then $e(k) \to 0$ exponentially, proving synchronization. □

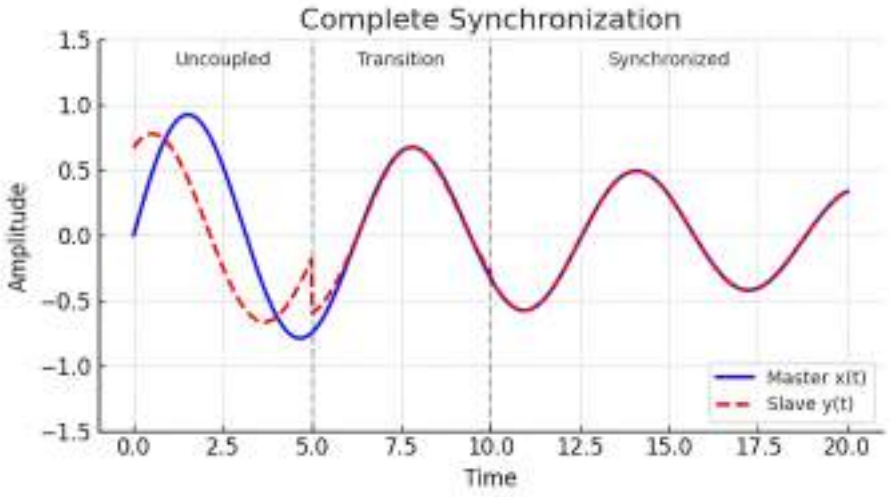


Figure 4.1: Complete Synchronization Diagram

Example:

Consider the discrete-time Hénon map as master system:

$$\begin{cases} x_1(k+1) &= 1 - \alpha x_1^2(k) + x_2(k) \\ x_2(k+1) &= \beta x_1(k) \end{cases} \tag{4.13}$$

with $\alpha = 1.4$, $\beta = 0.3$ and slave system:

$$\begin{cases} y_1(k+1) &= 1 - \alpha y_1^2(k) + y_2(k) + K[x_1(k) - y_1(k)] \\ y_2(k+1) &= \beta y_1(k) \end{cases} \tag{4.14}$$

where K is the coupling strength. For $K > 0.5$, the error dynamics

$$e_i(k) = y_i(k) - x_i(k) \tag{4.15}$$

evolve as

$$\begin{aligned} e_1(k+1) &= -\alpha[y_1^2(k) - x_1^2(k)] + e_2(k) - Ke_1(k) \\ &= -\alpha[y_1(k) + x_1(k)]e_1(k) + e_2(k) - Ke_1(k) \\ e_2(k+1) &= \beta e_1(k) \end{aligned} \tag{4.16}$$

The error system has the fixed point $(0, 0)$ which becomes stable when K exceeds the critical coupling strength, leading to

$$\lim_{k\to\infty} \|Y(k) - X(k)\| = 0 \tag{4.17}$$

4.3.2 Anti-Synchronization

Definition 4.5. [25] Two chaotic systems achieve anti-synchronization when:

$$\lim_{k\to\infty} \|Y(k) + X(k)\| = 0 \tag{4.18}$$

Theorem 4.2 (**Anti-Synchronization Theorem**). *[25] Consider two coupled chaotic systems:*

$$\dot{X} = F(X), \quad \dot{Y} = G(Y) + U \tag{4.19}$$

where $F = G$. If there exists a coupling U such that all conditional Lyapunov exponents of the anti-synchronization error $e(t) = Y(t) + X(t)$ are negative, then:

$$\lim_{t\to\infty} \|Y(t) + X(t)\| = 0. \tag{4.20}$$

Proof. Define the error:

$$e(t) = Y(t) + X(t). \tag{4.21}$$

Differentiating:

$$\dot{e}(t) = G(Y(t)) + G(X(t)) + U. \tag{4.22}$$

Let the control input be:

$$U = -G(Y(t)) - G(X(t)) - Ke(t), \tag{4.23}$$

with K positive definite. Then:

$$\dot{e}(t) = -Ke(t). \tag{4.24}$$

Define the Lyapunov function:

$$V(e) = \frac{1}{2}e^T e, \quad \dot{V}(e) = -e^T Ke < 0 \quad \forall e \neq 0. \tag{4.25}$$

Hence, $e(t) \to 0$ as $t \to \infty$, proving anti-synchronization. □

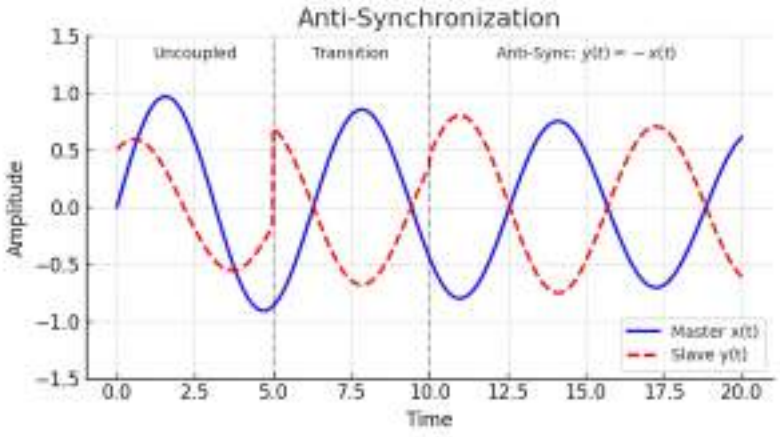


Figure 4.2: Anti Synchronization Diagram

Example:

Consider two coupled Lorenz systems. The master system is given by:

$$\begin{cases} \dot{x}_1 &= \sigma(x_2 - x_1) \\ \dot{x}_2 &= x_1(\rho - x_3) - x_2 \\ \dot{x}_3 &= x_1 x_2 - \beta x_3 \end{cases} \tag{4.26}$$

and the slave system is:

$$\begin{cases} \dot{y}_1 &= \sigma(y_2 - y_1) + K_1(x_1 + y_1) \\ \dot{y}_2 &= y_1(\rho - y_3) - y_2 + K_2(x_2 + y_2) \\ \dot{y}_3 &= y_1 y_2 - \beta y_3 + K_3(x_3 + y_3) \end{cases} \tag{4.27}$$

with $\sigma = 10$, $\rho = 28$, and $\beta = \frac{8}{3}$. Defining the anti-synchronization error as:

$$e_i = y_i + x_i \tag{4.28}$$

the error dynamics become:

$$\begin{aligned} \dot{e}_1 &= \sigma(e_2 - e_1) + K_1 e_1 + 2\sigma x_2 - 2\sigma x_1 \\ \dot{e}_2 &= \rho e_1 - e_2 - y_1 y_3 - x_1 x_3 + K_2 e_2 \\ \dot{e}_3 &= y_1 y_2 + x_1 x_2 - \beta e_3 + K_3 e_3 \end{aligned} \tag{4.29}$$

For gain values $K_1 = -15$, $K_2 = 0$, and $K_3 = -1$, the Lyapunov function

$$V = \frac{1}{2}(e_1^2 + e_2^2 + e_3^2) \tag{4.30}$$

guarantees $\dot{V} < 0$ when $\|e\|$ is sufficiently large, ensuring:

$$\lim_{t\to\infty} \|Y(t) + X(t)\| = 0 \tag{4.31}$$

4.3.3 Phase Synchronization

Definition 4.6. [16] Two chaotic systems achieve phase synchronization when their phases lock while amplitudes remain uncorrelated:

$$\lim_{k\to\infty} |\varphi_Y(k) - \varphi_X(k)| = 0 \tag{4.32}$$

where φ_X and φ_Y represent the phases of systems X and Y.

Theorem 4.3 (**Phase Synchronization Theorem**). *Let $(X(t), Y(t))$ be trajectories of two weakly coupled chaotic oscillators with natural frequencies ω_1 and ω_2. If the coupling strength ϵ exceeds the critical value $\epsilon_c \propto |\omega_1 - \omega_2|$, then phase synchronization occurs:*

$$|\varphi_Y(t) - \varphi_X(t)| < C \quad \textit{for all } t > T_0. \tag{4.33}$$

Proof. Phase difference dynamics follow the stochastic Adler equation:

$$\frac{d\Delta\varphi}{dt} = \Delta\omega - \epsilon \sin(\Delta\varphi) + \xi(t), \tag{4.34}$$

where $\Delta\varphi = \varphi_Y - \varphi_X$, $\Delta\omega = \omega_2 - \omega_1$, and $\xi(t)$ are fluctuations. In the deterministic case ($\xi(t) = 0$), locking occurs if:

$$|\Delta\omega| < \epsilon. \tag{4.35}$$

In the stochastic case, the condition becomes:

$$\epsilon > \epsilon_c = |\Delta\omega| + \sigma_\xi, \tag{4.36}$$

where σ_ξ quantifies fluctuations. Phase synchronization implies equal time-averaged frequencies:

$$\Omega_X = \lim_{T\to\infty} \frac{\varphi_X(T) - \varphi_X(0)}{T}, \quad \Omega_Y = \lim_{T\to\infty} \frac{\varphi_Y(T) - \varphi_Y(0)}{T}, \tag{4.37}$$

with $\Omega_X = \Omega_Y$, hence bounded phase difference. □

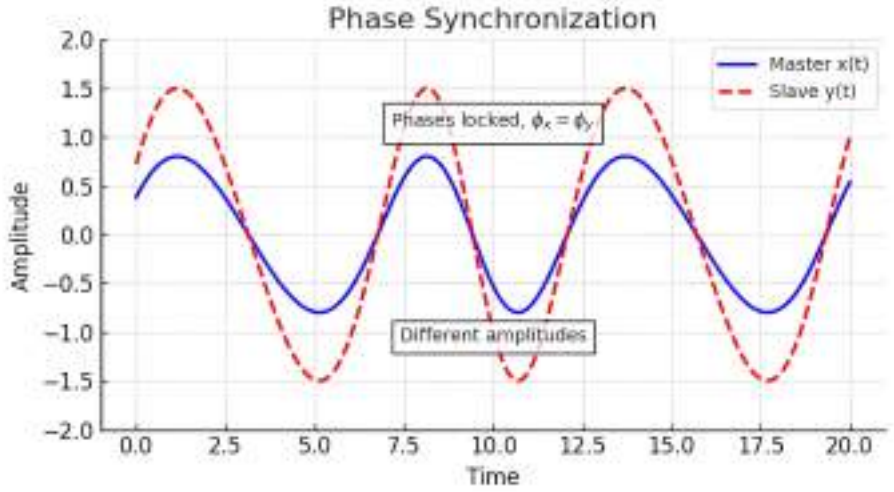


Figure 4.3: Phase Synchronization Diagram

Example:

Consider two coupled Rössler systems with different frequencies:

$$\begin{cases} \dot{x}_1 &= -\omega_x x_2 - x_3 \\ \dot{x}_2 &= \omega_x x_1 + 0.15 x_2 \\ \dot{x}_3 &= 0.2 + x_3(x_1 - 10) \end{cases} \tag{4.38}$$

and

$$\begin{cases} \dot{y}_1 &= -\omega_y y_2 - y_3 + \epsilon(x_1 - y_1) \\ \dot{y}_2 &= \omega_y y_1 + 0.15 y_2 \\ \dot{y}_3 &= 0.2 + y_3(y_1 - 10) \end{cases} \tag{4.39}$$

with $\omega_x = 0.98$, $\omega_y = 1.02$. The phase can be defined as

$$\varphi_x(t) = \arctan(x_2/x_1), \quad \varphi_y(t) = \arctan(y_2/y_1) \tag{4.40}$$

For coupling strength $\epsilon > \epsilon_c \approx 0.037$, phase locking occurs where

$$|\varphi_y(t) - \varphi_x(t)| < \text{constant} \tag{4.41}$$

for all t, while the amplitudes

$$r_x = \sqrt{x_1^2 + x_2^2}, \quad r_y = \sqrt{y_1^2 + y_2^2} \tag{4.42}$$

remain uncorrelated with correlation coefficient

$$\rho(r_x, r_y) \ll 1 \tag{4.43}$$

4.3.4 Lag Synchronization

Definition 4.7. [16] Two systems exhibit lag synchronization when one system follows the dynamics of the other with a constant time delay $\tau > 0$:

$$\lim_{k\to\infty} \|Y(k) - X(k-\tau)\| = 0 \tag{4.44}$$

Theorem 4.4 (**Lag Synchronization Theorem**). *Let $X(t)$ and $Y(t)$ be two coupled chaotic systems with a constant time delay $\tau > 0$. If the coupling ensures that*

$$\lim_{t\to\infty} \|Y(t) - X(t-\tau)\| = 0, \tag{4.45}$$

then lag synchronization is achieved.

Proof. Define the lag error:

$$e(t) = Y(t) - X(t-\tau). \tag{4.46}$$

Assume $Y(t)$ is driven by $X(t-\tau)$ through coupling:

$$\dot{Y}(t) = F(Y(t)) + K(X(t-\tau) - Y(t)), \tag{4.47}$$

with K a positive definite matrix. Then:

$$\dot{e}(t) = \dot{Y}(t) - \dot{X}(t-\tau) = F(Y(t)) - F(X(t-\tau)) + Ke(t). \tag{4.48}$$

Assuming Lipschitz continuity of F:

$$\|\dot{e}(t)\| \leq L\|e(t)\| - \lambda\|e(t)\|, \tag{4.49}$$

for some $L < \lambda$. Then $e(t) \to 0$, hence lag synchronization occurs. □

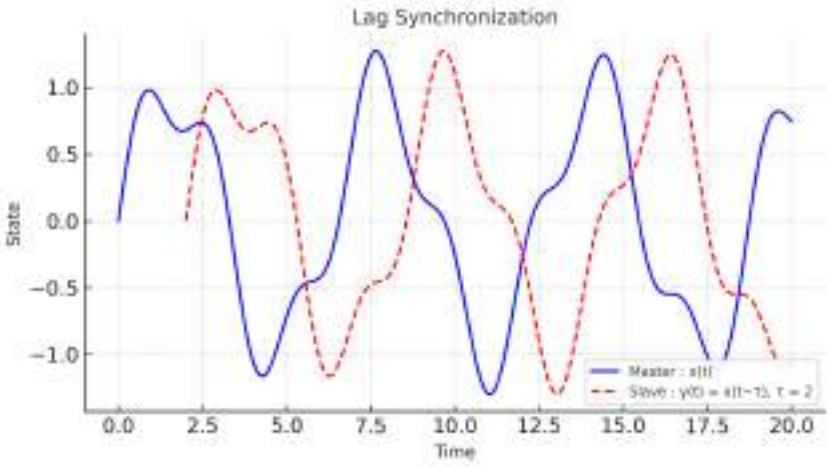


Figure 4.4: Lag Synchronization Diagram

Example:

Consider unidirectionally coupled Rössler systems with parameter mismatch. The master system is defined as:

$$\begin{cases} \dot{x}_1 &= -\omega_1 x_2 - x_3 \\ \dot{x}_2 &= \omega_1 x_1 + 0.15 x_2 \\ \dot{x}_3 &= 0.2 + x_3(x_1 - 10) \end{cases} \tag{4.50}$$

and the slave system is given by:

$$\begin{cases} \dot{y}_1 &= -\omega_2 y_2 - y_3 + K(x_1 - y_1) \\ \dot{y}_2 &= \omega_2 y_1 + 0.15 y_2 \\ \dot{y}_3 &= 0.2 + y_3(y_1 - 10) \end{cases} \tag{4.51}$$

with $\omega_1 = 1.0$, $\omega_2 = 0.95$. For moderate coupling $K \approx 0.15$, the similarity function:

$$S_2(\tau) = \frac{\langle [Y(t+\tau) - X(t)]^2 \rangle}{\langle X^2(t) \rangle \langle Y^2(t) \rangle} \tag{4.52}$$

has a minimum at $\tau \approx 0.25$, indicating that $Y(t+\tau) \approx X(t)$, or equivalently $Y(t) \approx X(t-\tau)$. The time series analysis shows that the normalized lag synchronization error:

$$\frac{\|Y(k) - X(k-\tau)\|}{\|X(k-\tau)\|} < 0.05 \quad \text{for} \quad k > k_0 \tag{4.53}$$

4.3.5 Generalized Synchronization

Definition 4.8. [11] Two possibly non-identical and different-dimensional systems achieve *generalized synchronization* when there exists a functional relationship between their states:

$$\exists\, \varphi : \mathbb{R}^n \to \mathbb{R}^m \quad \text{such that} \quad \lim_{k\to\infty} \|Y(k) - \varphi(X(k))\| = 0 \tag{4.54}$$

Theorem 4.5 (**Generalized Synchronization Theorem**). *[11] Let $X(k)$ and $Y(k)$ be chaotic systems with dynamics:*

$$X(k+1) = F(X(k)), \quad Y(k+1) = G(Y(k), X(k)), \tag{4.55}$$

If there exists a smooth function Φ such that:

$$\lim_{k\to\infty} \|Y(k) - \Phi(X(k))\| = 0, \tag{4.56}$$

then Y is in generalized synchronization with X.

Proof. Define the synchronization manifold:

$$M = \{(X, Y) \in \mathbb{R}^n \times \mathbb{R}^m \mid Y = \Phi(X)\}. \tag{4.57}$$

Let the error be:

$$e(k) = Y(k) - \Phi(X(k)). \tag{4.58}$$

Differentiating:

$$e(k+1) = G(Y(k), X(k)) - \Phi(F(X(k))). \tag{4.59}$$

If the composite map $G(Y, X)$ is contracting in Y near M and Φ is stable under F, then $e(k) \to 0$ by the contraction mapping principle. Hence generalized synchronization occurs. □

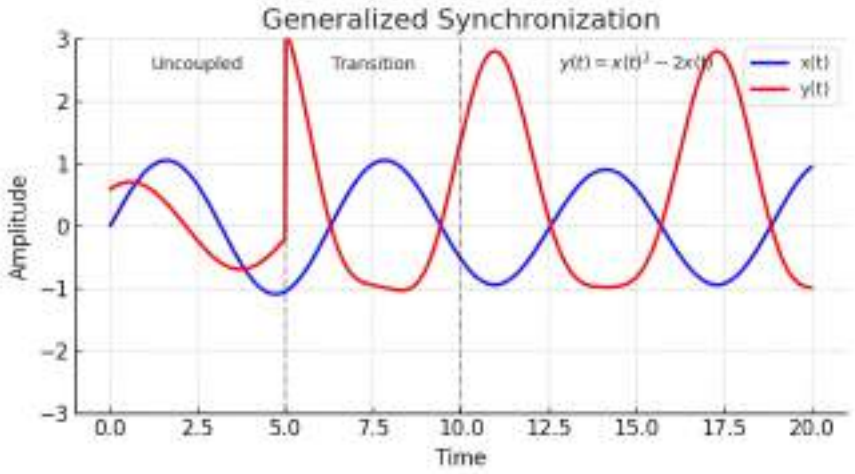


Figure 4.5: Generalized Synchronization Diagram

Example:

Consider a 3D *Rössler* system as the master system:

$$\begin{cases} \dot{x}_1 &= -x_2 - x_3 \\ \dot{x}_2 &= x_1 + 0.2x_2 \\ \dot{x}_3 &= 0.2 + x_3(x_1 - 5.7) \end{cases} \tag{4.60}$$

and a 4D hyperchaotic system as the response:

$$\begin{cases} \dot{y}_1 &= y_2 + y_3 \\ \dot{y}_2 &= -y_1 + 0.5y_2 + y_4 \\ \dot{y}_3 &= 3.0 + y_1 y_3 \\ \dot{y}_4 &= -0.5y_3 \end{cases} \tag{4.61}$$

The systems are coupled through a nonlinear function:

$$\dot{y}_1 = y_2 + y_3 + K[g_1(X) - y_1] \tag{4.62}$$

where

$$g_1(X) = x_1^2 - 2x_3 \tag{4.63}$$

is a nonlinear mapping. For coupling strength $K > K_c \approx 2.5$, the presence of generalized synchronization can be verified using the *auxiliary system approach*, by constructing an identical copy of the response system:

$$\begin{cases} \dot{z}_1 &= z_2 + z_3 + K[g_1(X) - z_1] \\ \dot{z}_2 &= -z_1 + 0.5z_2 + z_4 \\ \dot{z}_3 &= 3.0 + z_1 z_3 \\ \dot{z}_4 &= -0.5z_3 \end{cases} \tag{4.64}$$

with different initial conditions from the original system Y. If generalized synchronization occurs, then:

$$\lim_{t\to\infty} \|Y(t) - Z(t)\| = 0 \tag{4.65}$$

indicating that both response systems Y and Z evolve identically under the same driving signal X, confirming the existence of a functional relationship $\varphi(X)$.

4.3.6 Projective Synchronization

Definition 4.9. [7] Two systems achieve projective synchronization when the state variables of one system become proportional to the corresponding state variables of the other by constant scaling factors:

$$\exists\, \alpha_i \in \mathbb{R} : \lim_{k\to\infty} |y_i(k) - \alpha_i x_i(k)| = 0, \quad i = 1, \ldots, n \tag{4.66}$$

Theorem 4.6 (**Projective Synchronization Theorem**). *Let two systems be related as*

$$\dot{Y}(t) = F(Y(t)) + U(t), \quad \dot{X}(t) = F(X(t)), \tag{4.67}$$

and suppose there exists a scalar $\alpha \in \mathbb{R}$ such that:

$$\lim_{t\to\infty} \|Y(t) - \alpha X(t)\| = 0. \tag{4.68}$$

Then the systems are in projective synchronization.

Proof. Define the error:

$$e(t) = Y(t) - \alpha X(t). \tag{4.69}$$

Then:

$$\dot{e}(t) = \dot{Y}(t) - \alpha\dot{X}(t) = F(Y(t)) + U(t) - \alpha F(X(t)). \tag{4.70}$$

Using the coupling:

$$U(t) = -F(Y(t)) + \alpha F(X(t)) - Ke(t), \tag{4.71}$$

yields:

$$\dot{e}(t) = -Ke(t). \tag{4.72}$$

The Lyapunov function:

$$V(e) = \frac{1}{2}e^T e, \quad \dot{V} = -e^T Ke < 0 \quad \forall e \neq 0, \tag{4.73}$$

ensures convergence to $e(t) = 0$. Thus, $Y(t) = \alpha X(t)$ asymptotically. □

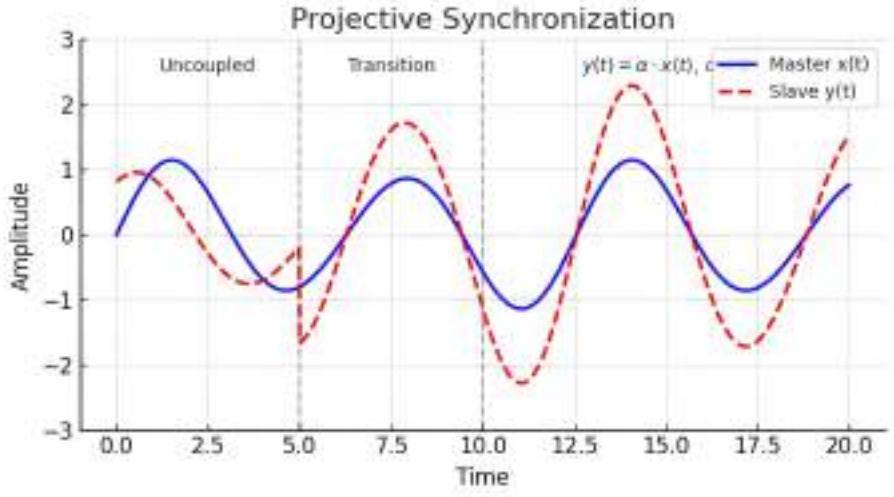


Figure 4.6: Projective Synchronization Diagram

Example:

Consider the master-slave configuration of the Lorenz system.
The master system is defined by:

$$\begin{cases} \dot{x}_1 &= \sigma(x_2 - x_1) \\ \dot{x}_2 &= x_1(\rho - x_3) - x_2 \\ \dot{x}_3 &= x_1 x_2 - \beta x_3 \end{cases} \tag{4.74}$$

and the slave system is given by:

$$\begin{cases} \dot{y}_1 &= \sigma(y_2 - y_1) + K_1(y_1 - \alpha_1 x_1) \\ \dot{y}_2 &= y_1(\rho - y_3) - y_2 + K_2(y_2 - \alpha_2 x_2) \\ \dot{y}_3 &= y_1 y_2 - \beta y_3 + K_3(y_3 - \alpha_3 x_3) \end{cases} \tag{4.75}$$

with parameters $\sigma = 10$, $\rho = 28$, $\beta = 8/3$ and scaling factors $\alpha_1 = \alpha_2 = \alpha_3 = 2$. Using control gains $K_1 = K_2 = K_3 = -15$, the scaling errors $e_i = y_i - \alpha_i x_i$ evolve according to:

$$\begin{aligned} \dot{e}_1 &= \sigma(e_2 - e_1) + K_1 e_1 \\ \dot{e}_2 &= \rho e_1 - e_2 - y_1 y_3 + \alpha_2 x_1 x_3 + K_2 e_2 \\ \dot{e}_3 &= y_1 y_2 - \alpha_3 x_1 x_2 - \beta e_3 + K_3 e_3 \end{aligned} \tag{4.76}$$

Numerical simulations confirm that:

$$\lim_{t \to \infty} |y_i(t) - 2x_i(t)| = 0, \quad i = 1, 2, 3 \tag{4.77}$$

indicating that the response system's trajectory is a scaled replica of the drive system with scaling factor 2.

4.3.7 Full State Hybrid Projective Synchronization (FSHPS)

Definition 4.10. [13] Two systems achieve FSHPS when each state variable of one system synchronizes to a linear combination of all state variables of the other system:

$$\exists(\beta_{ij}) \in \mathbb{R}^{n\times n} : \lim_{k\to\infty} \|y_i(k) - \sum_{j=1}^{n} \beta_{ij} x_j(k)\| = 0, \quad i = 1, \ldots, n \tag{4.78}$$

Theorem 4.7 (**FSHPS Theorem**). *[13] Let drive and response systems be described by:*

$$\dot{X}(t) = A(X(t)), \quad \dot{Y}(t) = B(Y(t)) + U(t), \tag{4.79}$$

where $U(t)$ is designed such that

$$\lim_{t\to t_f} \|Y(t) - PX(t)\| = 0, \tag{4.80}$$

for some diagonal matrix P and finite $t_f > 0$. Then the systems achieve finite-time stable hybrid projective synchronization.

Proof. [13] Define the error:

$$e(t) = Y(t) - PX(t). \tag{4.81}$$

Suppose $U(t)$ is chosen as:

$$U(t) = -B(Y(t)) + PA(X(t)) - Ke(t)^{\beta}, \quad 0 < \beta < 1. \tag{4.82}$$

Then:

$$\dot{e}(t) = -Ke(t)^{\beta}. \tag{4.83}$$

This nonlinear differential equation ensures that $e(t)$ reaches zero in finite time. Let $V = \frac{1}{2}\|e(t)\|^2$, then:

$$\dot{V} = -K'V^{\beta}, \quad \text{for some } K' > 0. \tag{4.84}$$

Solving yields:

$$V(t) = \left(V(0)^{1-\beta} - K'(1-\beta)t\right)^{\frac{1}{1-\beta}}, \tag{4.85}$$

which reaches zero in finite time $t_f = \frac{V(0)^{1-\beta}}{K'(1-\beta)}$. □

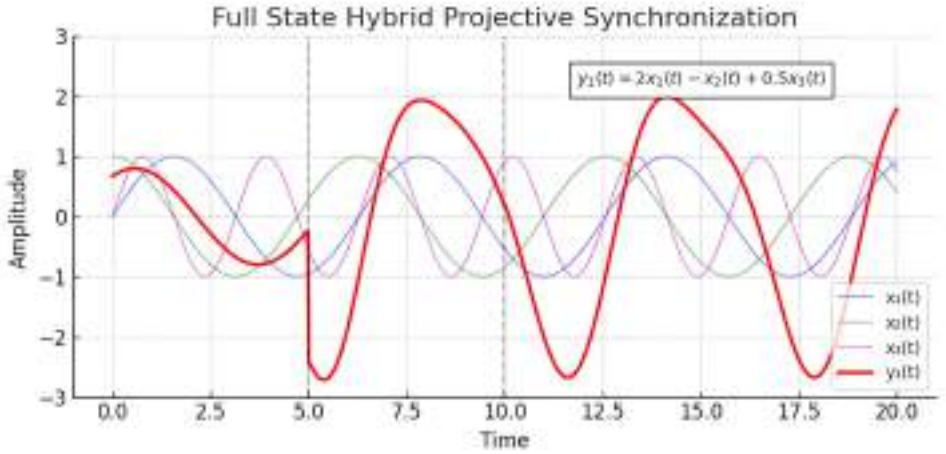


Figure 4.7: FSHP Synchronization Diagram

Example:

Consider the following master-slave configuration of the 3-dimensional Lu system:

$$\begin{cases} \dot{x}_1 &= a(x_2 - x_1) \\ \dot{x}_2 &= -x_1 x_3 + c x_2 \\ \dot{x}_3 &= x_1 x_2 - b x_3 \end{cases} \tag{4.86}$$

and the slave system is governed by:

$$\begin{cases} \dot{y}_1 &= a(y_2 - y_1) + u_1 \\ \dot{y}_2 &= -y_1 y_3 + c y_2 + u_2 \\ \dot{y}_3 &= y_1 y_2 - b y_3 + u_3 \end{cases} \tag{4.87}$$

with parameters $a = 36$, $b = 3$, and $c = 20$. The control inputs u_i are designed to achieve FSHPS with the scaling matrix

$$\beta = \begin{pmatrix} 2 & -1 & 0.5 \\ 1 & 3 & 0 \\ -0.5 & 0 & 2 \end{pmatrix}. \tag{4.88}$$

Define the error terms as

$$e_i = y_i - \sum_{j=1}^{3} \beta_{ij} x_j. \tag{4.89}$$

The controllers are defined as:

$$\begin{aligned} u_1 &= -a(y_2 - y_1) + a\beta_{11}(x_2 - x_1) + a\beta_{12}x_2 + a\beta_{13}x_3 - \lambda_1 e_1, \\ u_2 &= y_1 y_3 - c y_2 + \beta_{21}(-x_1 x_3 + c x_1) + \beta_{22}(-x_2 x_3 + c x_2) + \beta_{23}(-x_3 x_3 + c x_3) - \lambda_2 e_2, \\ u_3 &= -y_1 y_2 + b y_3 + \beta_{31} x_1 x_2 - \beta_{31} b x_1 + \beta_{32} x_2 x_2 - \beta_{32} b x_2 + \beta_{33} x_3 x_2 - \beta_{33} b x_3 - \lambda_3 e_3. \end{aligned} \tag{4.90}$$

where $\lambda_i > 0$ are control gains. With these controllers, the error dynamics become:

$$\dot{e}_i = -\lambda_i e_i, \tag{4.91}$$

which ensures that:

$$\lim_{t\to\infty} \|e_i(t)\| = 0. \tag{4.92}$$

This implies the following synchronization:

$$\lim_{t\to\infty} \|Y(t) - \varphi(X(t))\| = 0. \tag{4.93}$$

4.3.8 Q-S Synchronization

Definition 4.11. [25] Two systems achieve *Q-S synchronization* when there exist transformation functions Q and S such that the transformed states become identical:

$$\exists\, Q : \mathbb{R}^n \to \mathbb{R}^d,\ S : \mathbb{R}^m \to \mathbb{R}^d \quad \text{such that} \quad \lim_{k\to\infty} \|Q(X(k)) - S(Y(k))\| = 0 \tag{4.94}$$

Theorem 4.8 (**Q–S Synchronization Theorem**). *[25] Let systems $X(k)$ and $Y(k)$ satisfy:*

$$X(k+1) = F(X(k)), \quad Y(k+1) = G(Y(k), X(k)), \tag{4.95}$$

and suppose there exist smooth functions $S(\cdot)$ and $Q(\cdot)$ such that:

$$\lim_{k\to\infty} \|S(Y(k)) - Q(X(k))\| = 0. \tag{4.96}$$

Then the systems achieve S–Q synchronization.

Proof. Let the synchronization error be:

$$e(k) = S(Y(k)) - Q(X(k)). \tag{4.97}$$

Assume the following control law:

$$Y(k+1) = G(Y(k)) - K \cdot \nabla S(Y(k))^T e(k), \tag{4.98}$$

where K is a gain matrix and ∇S is the Jacobian of S. Then:

$$e(k+1) = S(Y(k+1)) - Q(X(k+1)). \tag{4.99}$$

Under regularity and contraction assumptions on S, Q, and G, we obtain:

$$\|e(k+1)\| < \|e(k)\|, \quad \text{so} \quad e(k) \to 0, \tag{4.100}$$

which yields $S(Y(k)) \to Q(X(k))$, hence S–Q synchronization. □

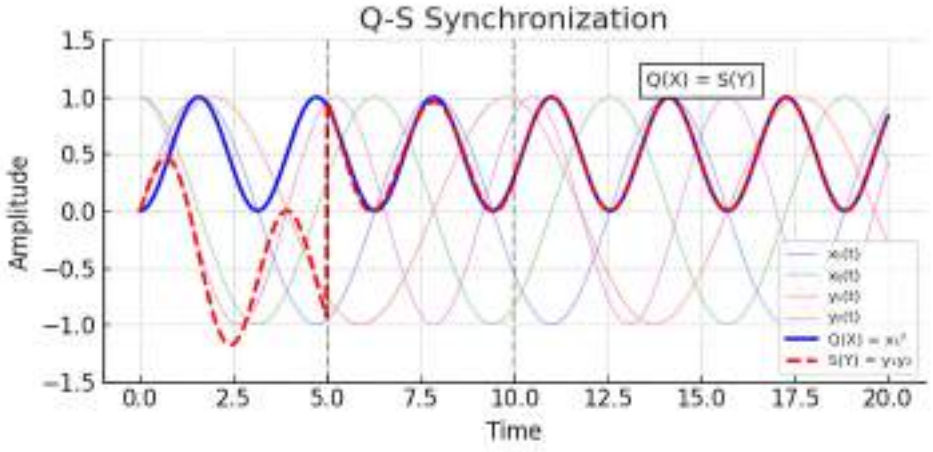


Figure 4.8: Q-S Synchronization Diagram

Example:

Consider the *Lorenz* system as the drive system:

$$\begin{cases} \dot{x}_1 &= \sigma(x_2 - x_1) \\ \dot{x}_2 &= x_1(\rho - x_3) - x_2 \\ \dot{x}_3 &= x_1 x_2 - \beta x_3 \end{cases} \tag{4.101}$$

with parameters $\sigma = 10$, $\rho = 28$, and $\beta = \frac{8}{3}$.

Let the response system be the *Chen* system with control inputs:

$$\begin{cases} \dot{y}_1 &= a(y_2 - y_1) + u_1 \\ \dot{y}_2 &= (c - a)y_1 - y_1 y_3 + c y_2 + u_2 \\ \dot{y}_3 &= y_1 y_2 - b y_3 + u_3 \end{cases} \tag{4.102}$$

with parameters $a = 35$, $b = 3$, and $c = 28$.

Define the transformation functions:

$$Q(X) = \left(x_1^2,\, x_2 - x_3,\, x_1 + x_3\right) \tag{4.103}$$

$$S(Y) = (y_1 y_3,\, y_2 + y_3,\, 2y_1 - y_2) \tag{4.104}$$

Design the control inputs to enforce convergence:

$$\begin{aligned} u_1 &= -a(y_2 - y_1) + y_3\left[-\dot{q}_1 + \lambda_1(q_1 - s_1)\right] \\ u_2 &= -(c - a)y_1 + y_1 y_3 - c y_2 + \left[\dot{q}_2 + \dot{q}_3 + \lambda_2(q_2 - s_2) + \lambda_3(q_3 - s_3)\right] \\ u_3 &= -y_1 y_2 + b y_3 + \left[\dot{q}_2 - \dot{q}_3 + \lambda_2(q_2 - s_2) - \lambda_3(q_3 - s_3)\right] \end{aligned} \tag{4.105}$$

where q_i and s_i are the components of $Q(X)$ and $S(Y)$, respectively, and $\lambda_i > 0$ are positive constants.

Define the synchronization error:

$$e_i = q_i - s_i \tag{4.106}$$

which evolves according to the linear system:

$$\dot{e}_i = -\lambda_i e_i \tag{4.107}$$

ensuring exponential decay:

$$\|Q(X(t)) - S(Y(t))\| \to 0 \quad \text{as} \quad t \to \infty \tag{4.108}$$

Numerical simulations confirm that after transient dynamics vanish:

$$x_1^2 \approx y_1 y_3, \quad x_2 - x_3 \approx y_2 + y_3, \quad x_1 + x_3 \approx 2y_1 - y_2 \tag{4.109}$$

verifying that Q-S synchronization has been achieved.

4.4 Methods of Synchronization

4.4.1 Active Controller Method

The application of active control for the synchronization of chaotic systems was proposed by Bai and Lonngren. It is an effective technique that has demonstrated its power not only for synchronizing identical systems but also for synchronizing non-identical systems. Moreover, this method offers remarkable simplicity in algorithm implementation. [28]

Let two chaotic systems to be synchronized—master and slave—be defined by:

$$\begin{aligned} x(k+1) &= F\big(x(k)\big), \\ y(k+1) &= G\big(y(k)\big) + U, \end{aligned} \tag{4.110}$$

where :

- $x(k)$, $y(k) \in \mathbb{R}^n$ are the states of the master and slave systems, respectively.
- $F : \mathbb{R}^n \to \mathbb{R}^n$ and $G : \mathbb{R}^n \to \mathbb{R}^n$ are known mappings.
- $U = (u_i(k))_{1 \le i \le n}$ is the controller to be determined.

For the two systems to synchronize, the error between their trajectories must converge to zero as time tends to infinity. This error is defined by:

$$\begin{aligned} e(k+1) &= y(k+1) - x(k+1) \\ &= G\big(y(k)\big) - F\big(x(k)\big) + U. \end{aligned} \tag{4.111}$$

If one can write

$$G\big(y(k)\big) - F\big(x(k)\big) = A\, e(k) + N\big(x(k), y(k)\big), \tag{4.112}$$

where A is a constant $n \times n$ matrix and N is a nonlinear function, then

$$e(k+1) = A\, e(k) + N\big(x(k), y(k)\big) + U. \tag{4.113}$$

The active controller U is chosen as

$$U = -\,N\big(x(k), y(k)\big) + V, \tag{4.114}$$

where V is a linear term defined by

$$V = -L\,e(k), \tag{4.115}$$

and L is an $n \times n$ gain matrix. Substituting, the error evolves according to

$$e(k+1) = \big(A - L\big)\,e(k). \tag{4.116}$$

Thus, the synchronization problem for the master system $x(k+1) = F\big(x(k)\big)$ and the slave system $y(k+1) = G\big(y(k)\big) + U$ reduces to the problem of zero-stabilizing the linear discrete system

$$e(k+1) = \big(A - L\big)\,e(k). \tag{4.117}$$

Example:

Consider the master and slave systems described by the logistic map:

$$\begin{aligned} x_{k+1} &= r\,x_k\,(1 - x_k), \\ y_{k+1} &= r\,y_k\,(1 - y_k) + u_k, \end{aligned} \tag{4.118}$$

where x_k and y_k are in the interval $(0, 1)$, and $r = 3.9$ for chaotic behavior. Define the synchronization error as $e_k = y_k - x_k$. Then, we compute the evolution of the error:

$$e_{k+1} = y_{k+1} - x_{k+1} = r\,y_k(1 - y_k) - r\,x_k(1 - x_k) + u_k. \tag{4.119}$$

Simplifying the first two terms:

$$r\,y_k(1 - y_k) - r\,x_k(1 - x_k) = r\big[y_k - x_k - (y_k^2 - x_k^2)\big] = r\,(1 - x_k - y_k)\,e_k. \tag{4.120}$$

Thus, the error dynamics are:

$$e_{k+1} = A_k\,e_k + u_k, \quad \text{where} \quad A_k = r(1 - x_k - y_k). \tag{4.121}$$

To cancel the time-varying gain A_k, we introduce a constant contraction factor $\alpha \in (-1, 1)$, choosing:

$$u_k = -A_k\,e_k + \alpha\,e_k. \tag{4.122}$$

Substituting this into the error equation:

$$e_{k+1} = A_k\,e_k + (-A_k\,e_k + \alpha\,e_k) = \alpha\,e_k. \tag{4.123}$$

For $\alpha = 0.5$, the error evolves as:

$$e_{k+1} = 0.5\,e_k, \tag{4.124}$$

which ensures exponential convergence of the error to zero, meaning the slave system synchronizes with the master.

4.4.2 Adaptive Controller Method

The application of adaptive control for the synchronization of chaotic systems is particularly suitable when the system parameters are unknown or time-varying. This method offers the advantage of online parameter estimation, allowing synchronization even under model uncertainty. [27]

Let the master and slave chaotic systems be defined by:

$$\begin{aligned} x(k+1) &= F\big(x(k)\big), \\ y(k+1) &= G_0\big(y(k)\big) + \Phi\big(y(k)\big)\,\theta(k) + U(k), \end{aligned} \tag{4.125}$$

where :

- $x(k)$, $y(k) \in \mathbb{R}^n$ are the states of the master and slave systems, respectively.
- $F : \mathbb{R}^n \to \mathbb{R}^n$ is a known mapping.
- $\Phi(y(k)) \in \mathbb{R}^{n\times m}$ is a known regressor matrix.
- $\theta(k) \in \mathbb{R}^m$ is a vector of unknown or time-varying parameters.
- $U(k) \in \mathbb{R}^n$ is the control input to be determined.

The synchronization error is defined by:

$$\begin{aligned} e(k+1) &= y(k+1) - x(k+1) \\ &= G_0\big(y(k)\big) + \Phi\big(y(k)\big)\,\theta(k) + U(k) - F\big(x(k)\big). \end{aligned} \tag{4.126}$$

The adaptive control law is chosen as:

$$U(k) = -\,\Phi\big(y(k)\big)\,\hat{\theta}(k) - L\,e(k), \tag{4.127}$$

where :

- $\hat{\theta}(k)$ is the estimated parameter vector.
- $L \in \mathbb{R}^{n\times n}$ is a gain matrix to be designed.

Substituting the control input into the error equation yields:

$$e(k+1) = G_0\big(y(k)\big) - F\big(x(k)\big) + \Phi\big(y(k)\big)\,\Big(\theta(k) - \hat{\theta}(k)\Big) - L\,e(k). \tag{4.128}$$

To ensure convergence of the error to zero, the parameter estimate $\hat{\theta}(k)$ is updated using the adaptation law:

$$\hat{\theta}(k+1) = \hat{\theta}(k) + \Gamma\,\Phi^{\top}\big(y(k)\big)\,e(k), \tag{4.129}$$

where $\Gamma \in \mathbb{R}^{m\times m}$ is a positive definite adaptation gain matrix.

Under appropriate conditions on $\Phi(y(k))$, L, and Γ, the synchronization error $e(k)$ converges to zero as $k \to \infty$, and the parameter estimates $\hat{\theta}(k)$ converge to the true values $\theta(k)$.

Thus, the synchronization problem for the master system $x(k+1) = F\big(x(k)\big)$ and the slave system $y(k+1) = G_0\big(y(k)\big) + \Phi\big(y(k)\big)\,\theta(k) + U(k)$ reduces to the problem of stabilizing the error system with simultaneous parameter adaptation.

Example:

Now, suppose the slave system has an unknown parameter θ:

$$\begin{aligned} x_{k+1} &= r\, x_k\,(1 - x_k), \quad \text{(master, with known } r = 3.9), \\ y_{k+1} &= \theta\, y_k\,(1 - y_k) + u_k, \quad \text{(slave, with unknown } \theta). \end{aligned} \tag{4.130}$$

Define the synchronization error as:

$$e_k = y_k - x_k, \tag{4.131}$$

and the estimation error as:

$$\tilde{\theta}_k = \theta - \hat{\theta}_k, \tag{4.132}$$

where $\hat{\theta}_k$ is our estimate of θ. The error dynamics become:

$$e_{k+1} = \theta\, y_k(1 - y_k) + u_k - r\, x_k(1 - x_k). \tag{4.133}$$

We introduce a control law based on the estimated θ:

$$u_k = -\hat{\theta}_k\, y_k(1 - y_k) - L\, e_k, \tag{4.134}$$

where $L \in (0, 1)$ is a design gain. Substituting into the error equation, we get:

$$e_{k+1} = \left(\theta - \hat{\theta}_k\right) y_k(1 - y_k) - L\, e_k = -L\, e_k + \tilde{\theta}_k\, \phi_k, \tag{4.135}$$

where $\phi_k = y_k(1 - y_k)$. To estimate θ, we adopt an adaptation law:

$$\hat{\theta}_{k+1} = \hat{\theta}_k + \Gamma\, \phi_k\, e_k, \tag{4.136}$$

where $\Gamma > 0$ is a tuning parameter. To analyze convergence, we define a Lyapunov-like function:

$$V_k = \frac{1}{2}\, e_k^2 + \frac{1}{2\Gamma}\, \tilde{\theta}_k^2. \tag{4.137}$$

By showing that:

$$V_{k+1} - V_k \leq -c\, e_k^2 \quad \text{for some } c > 0, \tag{4.138}$$

we conclude that both:

$$\lim_{k\to\infty} e_k = 0 \quad \text{and} \quad \lim_{k\to\infty} \tilde{\theta}_k = 0, \tag{4.139}$$

which means the slave system synchronizes with the master and the parameter θ is correctly estimated.

4.5 Summary

This chapter presented an overview of chaos synchronization in discrete dynamical systems. We began by introducing the concept and formal definition of synchronization, emphasizing its theoretical significance and practical applications. Various types of synchronization were classified, from basic forms like complete and anti-synchronization to advanced types such as FSHPS and Q-S synchronization. Additionally, we outlined key synchronization methods, namely the active and adaptive controller approaches. Overall, this chapter established a foundational understanding of how synchronization can be achieved and classified in chaotic discrete systems.

Conclusion and Open Perspectives

The synchronization of chaos in discrete dynamical systems represents a mathematically rich and practically significant area of study, lying at the intersection of nonlinear dynamics, control theory, and complex systems analysis. While continuous-time synchronization has received extensive attention over the past decades, discrete-time synchronization is comparatively less mature, with many foundational questions remaining open. This thesis has contributed to the mathematical formalization of synchronization types and methods in discrete systems, paving the way for future theoretical developments and applications.

From a theoretical standpoint, the interplay between the structure of chaotic maps and the emergence of synchronized behavior raises deep questions about *invariant manifolds*, *functional relationships between states*, and the *stability of coupled systems*. The classification of synchronization regimes—particularly in the presence of nonlinearity, time delays, or high dimensionality—remains incomplete. Existing frameworks often rely on system-specific conditions, and a generalized theory unifying these diverse synchronization types is still lacking.

On the methodological front, the design of controllers for synchronization—whether through active or adaptive schemes—requires precise knowledge of system parameters, which may not always be available. This leads to important open problems involving *robust synchronization*, *parameter identification*, and the *effect of noise and discretization errors*. The challenge of ensuring synchronization under partial observability or limited communication is also of practical relevance, especially in networked systems and digital communication environments.

Several promising avenues for future research emerge naturally:

- The construction of a unified variational or operator-theoretic framework that encompasses all known synchronization types in discrete settings.
- Analytical derivation of synchronization thresholds and bifurcation conditions in coupled chaotic maps.
- Exploration of synchronization in *non-smooth* or *hybrid discrete systems*, including systems with switching dynamics or piecewise-linear maps.
- Development of data-driven or machine learning-based controllers that can synchronize systems without explicit model knowledge.
- Investigation of *topological invariants* and *entropy measures* as indicators of synchronization quality and complexity.

In conclusion, while significant strides have been made in understanding and controlling chaos in discrete-time systems, synchronization remains a domain of dynamic exploration. The inherent unpredictability of chaos, when tamed through synchronization, offers not only theoretical beauty but also practical utility in secure communication, information processing, and artificial intelligence. As digital systems continue to expand in complexity and interconnection, the mathematical challenges posed by synchronization will only grow more relevant. Thus, the study of synchronization in discrete chaotic systems is not a closed chapter but rather a continually evolving dialogue between theory and application—one that is poised to inspire research and innovation for years to come.

Bibliography

[1] V. S. Afraimovich, N. N. Verichev, and M. I. Rabinovich, *Stochastic synchronization of oscillations in dissipative systems*, Radiophysics and Quantum Electronics, vol. 29, no. 9, pp. 795–803, 1986.

[2] Ö. Akgümüş, *Neimark–Sacker bifurcation and stability of a prey–predator system*, Unpublished manuscript, received June 18, 2020.

[3] G. Álvarez and S. Li, *Some basic cryptographic requirements for chaos-based cryptosystems*, International Journal of Bifurcation and Chaos, vol. 16, no. 8, pp. 2129–2151, 2006.

[4] B. Aulbach and B. Kieninger, *On three definitions of chaos*, Unpublished manuscript, received April 20, 2000; revised July 18, 2000.

[5] S. Banerjee, *Border collision bifurcation: theory and applications*, Department of Electrical Engineering, Indian Institute of Technology, Kharagpur.

[6] D. Baptista and R. Severino, *Symbolic dynamics and Lyapunov exponents for Lozi maps*, ESAIM: Proceedings, vol. 36, pp. 121–125, 2012.

[7] S. Boccaletti, J. Kurths, G. Osipov, D. L. Valladares, and C. S. Zhou, *The synchronization of chaotic systems*, Physics Reports, 2002. Received January 2, 2002.

[8] E. Boukhalfa and Z. Elhadj, *Existence of super chaotic attractors in a general piecewise smooth map of the plane*, Interdisciplinary Description of Complex Systems, vol. 12, no. 1, pp. 92–98, 2014.

[9] E. Boukhalfa and Y. Laskri, *Quasi-controlling of chaotic discrete dynamical systems*, Global Journal of Pure and Applied Mathematics, vol. 12, no. 5, pp. 4317–4323, 2016.

[10] E. Boukhalfa, *Sur le chaos et synchronisation dans les systèmes dynamiques discrets*, PhD thesis in Applied Mathematics, 2017.

[11] A. Gasri, A. Ouannas, K. S. Ojo, and V.-T. Pham, *Coexistence of generalized synchronization and inverse generalized synchronization between chaotic and hyperchaotic systems*, Nonlinear Analysis: Modelling and Control, vol. 23, no. 4, pp. 598–583, 2018.

[12] D. Hamri, *Control and synchronization of chaotic systems in dimension 3 or more*, Doctoral thesis, Option: Stationary Problems, 2023.

[13] F. Hannachi and R. Amira, *On the dynamics and FSHP synchronization of a new chaotic 3-D system with three nonlinearities*, Unpublished manuscript, received January 12, 2023; revised May 26, 2023.

[14] P. Hartman, *A lemma in the theory of structural stability of differential equations*, Proceedings of the American Mathematical Society, vol. 11, no. 4, pp. 610–620, 1960.

[15] M. Hénon, *A two-dimensional mapping with a strange attractor*, Communications in Mathematical Physics, vol. 50, pp. 69–77, 1976.

[16] L. Jouini, *Quantification et synchronisation de chaos dans les systèmes dynamiques discrets*, Thèse de Doctorat, Université de Tebessa, 2021.

[17] E. N. Lorenz, *The Essence of Chaos*, University of Washington Press, 1993.

[18] R. Lozi, *Survey of recent applications of the chaotic Lozi map*, Algorithms, 2023.

[19] M. Martelli, *Introduction to discrete dynamical systems and chaos*, California State University, 1999.

[20] R. M. May, *Simple mathematical models with very complicated dynamics*, Nature, vol. 261, pp. 459–467, 1976.

[21] A. Ouannas, *On full-state hybrid projective synchronization of general discrete chaotic systems*, Unpublished manuscript, received July 28, 2014; published October 14, 2014.

[22] A. Ouannas and M. M. Al-Sawalha, *On inverse full state hybrid projective synchronization of chaotic dynamical systems in discrete-time*, International Journal of Dynamics and Control, vol. 5, no. 2, pp. 252–258, 2017.

[23] A. Ouannas, G. Grassi, A. Karouma, T. Ziar, X. Wang, and V.-T. Pham, *New type of chaos synchronization in discrete-time systems: the F–M synchronization*, Open Physics, vol. 16, 2018. DOI: 10.1515/phys-2018-0025. Received November 21, 2017; accepted January 31, 2018.

[24] L. M. Pecora and T. L. Carroll, *Synchronization in chaotic systems*, Physical Review Letters, vol. 64, no. 8, pp. 821–824, 1990.

[25] L. M. Pecora and T. L. Carroll, *Synchronization of chaotic systems*, Chaos: An Interdisciplinary Journal of Nonlinear Science, published online April 16, 2015.

[26] N. F. Rulkov, M. M. Sushchik, L. S. Tsimring, and H. D. I. Abarbanel, *Generalized synchronization of chaos in directionally coupled chaotic systems*, Physical Review E, vol. 51, no. 2, pp. 980–994, 1995.

[27] T. S. Santos and F. H. T. Vieira, *An adaptive control approach for discrete-time systems with unknown backlash at the input*, Unpublished manuscript, UNICAMP and Universidade Federal de Goiás.

[28] U. E. Vincent, *Chaos synchronization using active control and backstepping control: a comparative analysis*, Unpublished manuscript, received September 29, 2007; revised March 22, 2008; published online June 2, 2008.

[29] H. Wen, *A review of the Hénon map and its physical interpretations*, Georgia Institute of Technology, April 21, 2014.

[30] T. Yamada and H. Fujisaka, *Stability theory of synchronized motion in coupled-oscillator systems*, Progress of Theoretical Physics, vol. 70, no. 5, pp. 1240–1248, 1983.

[31] T. Yang, *A survey of chaotic secure communication systems*, International Journal of Computational Cognition, vol. 2, no. 2, pp. 81–130, 2004.

[32] Z. Elhadj, *A new chaotic attractor from 2-D discrete mapping via border-collision period doubling scenario*, Discrete Dynamics in Nature and Society, vol. 2005, pp. 235–238, 2005.

[33] Z. Elhadj and H. Nasr E-ddine, *A generalized model of some Lorenz-type and quasi-attractors type strange attractors in three dimensional dynamical systems*, International Journal of Pure and Applied Mathematical Sciences, vol. 2, no. 1, pp. 67–76, 2005.